University of Cincinnati

Date: 11/8/2019

I, Ramakrishna Surya, hereby submit this original work as part of the requirements for the degree of Master of Science in Materials Science.

It is entitled:

Synthesis and Characterization of Polyimide/Polyacrylonitrile Blend

Student's name: **Ramakrishna Surya**

This work and its defense approved by:

Committee chair: Jude Iroh, Ph.D.

Committee member: Jonathan Nickels, Ph.D.

Committee member: Yoonjee Park, Ph.D.

36464

Synthesis and Characterization of Polyimide/Polyacrylonitrile blend

A Thesis Submitted to the Graduate School of the University of Cincinnati in partial fulfillment of the requirements for the degree of

Master of Science

in the program of Materials Science and Engineering

in the Department of Mechanical and Materials Engineering

of the College of Engineering and Applied Science

University of Cincinnati, Cincinnati, Ohio, USA

By

Ramakrishna Surya

Bachelor of Technology in Metallurgical and Materials Technology

MGIT, Hyderabad, India

Thesis advisor and Committee Chair: Jude O. Iroh, Ph.D.

November 2019

Abstract

In this project the effect of polyacrylonitrile (PAN) on thermal and mechanical properties of polyimide (PI) was studied. The aim of this study is to formulate multifunctional polyimide/polyacrylonitrile blend by combining excellent properties of polyimide such as high solvent and wear resistance, high dimensional stability, excellent thermal resistance and high modulus with the superior properties of polyacrylonitrile such as low density, thermal stability, high strength and modulus of elasticity. Polyacrylonitrile is a high-performance polymer that unlike others has the capability to form highly oriented molecular structure when subjected to a low temperature heat treatment. It has applications in ultra-filtration membranes, hollow fibers for reverse osmosis and fibers for textile. It is also pre-cursor material for the manufacture of carbon fibers which are characterized by high stiffness, high tensile strength, low weight, high chemical resistance, high temperature tolerance and low thermal expansion.

In this study, a polyimide blend containing different weight percentages of polyacrylonitrile (0.1, 0.5, 1, 5 and 10 wt%) was synthesized and cast into thin films and fully characterized. The degradation behavior of the blends was studied using Thermogravimetric Analysis (TGA) and Differential Scanning Calorimetry (DSC). Functional group analysis and the chemical structure of the blend was studied by using Fourier Transform Infrared Spectroscopy (FTIR). Dynamic Mechanical Analysis (DMA), was used to study the changes in the storage modulus and damping behavior of the blends as a function of temperature and composition. The morphology and microstructure of the blends was studied by using the optical microscope.

From FTIR, the degree of imidization of the blend containing 10 wt.% of PAN was determined to be 97.5%. DMS analysis show the Tg of the blend containing 10 wt.% of PAN

was to be ~370°C. While the blend containing 10wt% of PAN produced the highest Tg, the blend containing 1wt% of PAN showed the highest damping ability. Rate of change of enthalpy was calculated using Differential Scanning Calorimetry and it shows that increasing the amount of PAN in the blend resulted in a decreasing heat release. The percentage weight loss and char retention were calculated from the TGA curves. By utilizing the results obtained from these techniques, the PI/PAN blends suitability for thermo-mechanical applications is assessed.

Acknowledgment

Firstly, I would like to specially thank and express my deepfelt gratitude to my research advisor, Professor Jude Iroh. He has always helped me with my research and has helped me immensely in gaining the knowledge and understanding for performing this research.

I would like to thank my committee members Professor Yoonjee Park and Professor Jonathan Nickels who took time from their busy schedules to be a part of my work.

I would like to express my gratitude to my research group members Wajeeh Marashdeh, Caroline Akinyi, Sakshi Sathyanarayana, Suriya Sekar, Philip Joseph, Ruchinda Gooneratne, Shengdong Xiao and Chengming Deng for their help and inputs in making my work better.

I would like to take this opportunity to thank all the Professors who taught different courses during my masters - Professor Relva Buchanan, Professor Donglu Shi, Professor Vijay Vasudevan, Professor Ashley Paz y Puente and Professor David Kundrat. I would also like to thank Dr. Necati Kaval for his help with FT-IR training and samples analysis.

I would like to thank my family and friends for being there for me through thick and thin.

Contents

List of Abbreviations

PAA	Poly (amic acid)
PI	Polyimide
PAN	Polyacrylonitrile
PMDA	Pyromellitic dianhydride
ODA	4-4’ oxydianiline
NMP	N- methyl-pyrrolidone
FTIR	Fourier Transform Infrared Spectroscopy
DOI	Degree of Imidization
DMA	Dynamic mechanical analysis
DSC	Differential Scanning Calorimetry
TGA	Thermogravimetric analysis
LOI	Limited Oxygen Index
Tg	Glass Transition Temperature

List of Figures

List of Tables

List of Equations

Chapter 1

Introduction

1.1 Overview of Project

Polyimide-based blends, copolymers and composites have always been a research interest owing to its vast array of properties and its compatibility with other materials to formulate composites and blends. The incorporation of polyacrylonitrile (PAN) into Polyimide (PI) is known to have improved mechanical properties, thermal stability, modulus and is shown to have increased fire retardancy.

In this project the effect of addition of polyacrylonitrile on polyimide's structure, mechanical and thermal properties is studied. A solution of polyacrylonitrile in N- methyl pyrrolidone was mixed into synthesized poly (amic acid) to obtain blends with varying weight percentage of PAN.

1.2 Research objectives

The aim of this project is to successfully synthesize and characterize polyimide (PI), polyacrylonitrile (PAN) and its blends. Thermal characterization is done to study the effect of PAN on PI's thermal properties and to observe changes in thermal behavior. Fourier Transform Infrared Spectroscopy (FT-IR) is done to monitor structural changes and changes in degree of imidization. Dynamic mechanical analysis is performed to observe the viscoelastic behavior of the blend when compared to its constituent polymers.

1.3 Polyimide matrix

Polyimides (PI) are in the class of high-performance polymers due to the specific rigid heterocyclic structures in the backbone. Polyimides are used in applications such as packing materials, aerospace materials, circuit boards and interlayer dielectrics due to its good dielectric properties, flexibility, excellent thermal stability, high tensile strength and good solvent resistance [1-5].

Fully aromatic PIs have rigid chains and strong interchain interactions which result in poor solubility and non-melting characteristics thus having low processability. Polyimides are manufactured by polycondensation of an anhydride and an amine in the presence of a dipolar aprotic solvent such as such as N-methyl-2-pyrollidone (NMP) and dimethyl formamide (DMF). An amine group attacks one of the carbonyl groups in the anhydride moiety, which results in a displacement of the carboxylate functionality, after which there is a proton transfer resulting in the formation of the poly (amic acid) (PAA) precursor [2]. The rate of reaction is dependent on the basicity of the solvent as mentioned in Koton et al [65]. The formation of PAA is reversible and is shown to change back into its respective diamine and dianhydride. The forward rate constant is significantly higher than the reverse rate constant which causes the reaction to appear irreversible. Additionally, using pure reagents for PAA synthesis results in a very low reverse rate constant. [66-67]

Upon exposure to temperatures greater that 250°C, poly (amic acid) (PAA) undergoes cyclization at the -NH and -OH site to release water and form polyimide (PI). This process alternatively is known as imidization. The degree to which PAA imidizes determines several properties of polyimide such as glass transition temperature (Tg) and mechanical properties such

as stiffness and flexibility. [64] There is direct correlation of Tg to the curing temperature, meaning a higher curing temperature cure yield polyimide with a higher Tg [4]-[8].

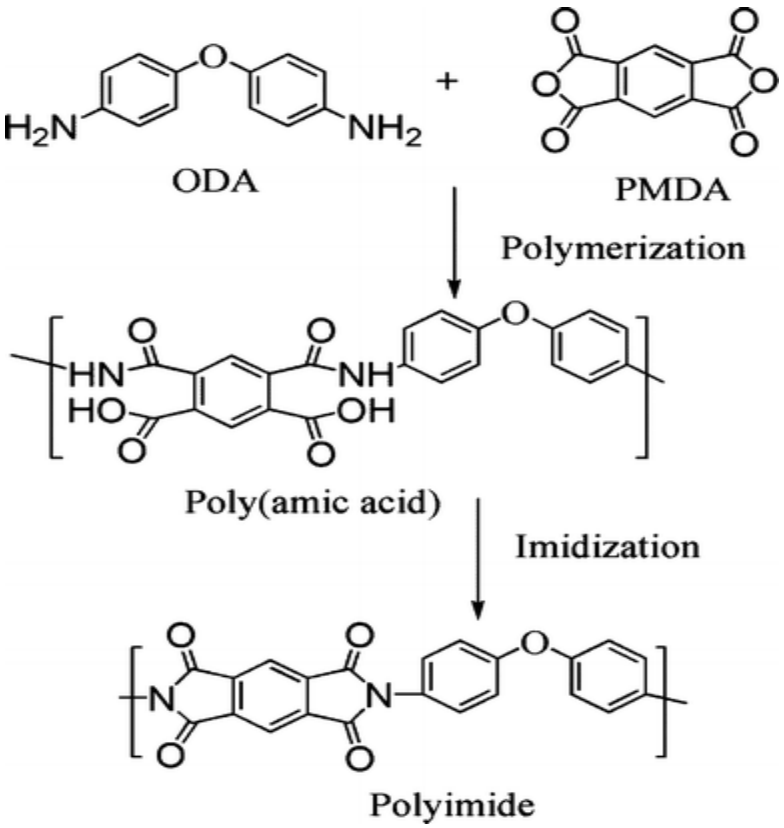

Figure 1: Schematic for the synthesis of Polyamic Acid from ODA and PMDA [2]

1.4 Polymer blends

Blending of polymers to improve final properties has always attracted both academic and industrial interest. Polymer blends exhibit a variety of improved properties such as strength and thermal resistance[11], improved solvent resistance[12], improved ionic [13] and electrical [14-17]conductivity, enhanced optical activity[18-21], flammability [22-25], decrease gas permeability [26-30] and increased modulus [31-35].

Several polymers have been used in the past as matrix materials for blend formulation. Rigid polymers such as polyimides [36-42], polyaniline [43], epoxy resins [44-47], poly (methyl methacrylate) [48-50] and butadiene acrylonitrile copolymer [51] are often used as host matrices. Parameters such as polymer-polymer compatibility, statistical thermodynamics, transport phenomena and phase separation behavior determine the ultimate properties of blends. Miscible polymers blends are expected to exhibit synergistic behavior where the addition of the second phase improves a property of the first polymer. Additionally, blending polymers from a commercial point of view provides cost dilution which can aid in engineering newer less expensive materials [52].

This study will focus on the effect of addition of polyacrylonitrile to polyimide matrix. The blend is then characterized for structural, thermal and mechanical properties.

1.5 Polyacrylonitrile

Polyacrylonitrile (PAN) is a semi crystalline organic polymer resin with a linear structure. Unlike other thermoplastics PAN degrades before melting under standard conditions. It has the capability to form highly oriented molecular structure when subjected to low temperature heat treatment. It has applications such as ultra-filtration membranes, hollow fibers for reverse

osmosis and fibers for textiles. Its low cost and high carbon yield make it highly favorable for manufacture of carbon fibers, which are formed when PAN is heated to a temperature of 300°C to form thermally stable ladder polymers and then carbonized at high temperatures (>1000°C). [54-57]

PAN homopolymers are used very infrequently owing to its poor processing properties, to counter this an appropriate amount of comonomer such as acrylic acid (AA), methacrylic acid (MAA) and itatonic acid (IA) is generally incorporated into PAN during polymerization for enhancing properties such as solubility, spinnability, hydrophilicity and drawability. This plays a crucial role in the properties and quality of resulting carbon fibers. [58,59]

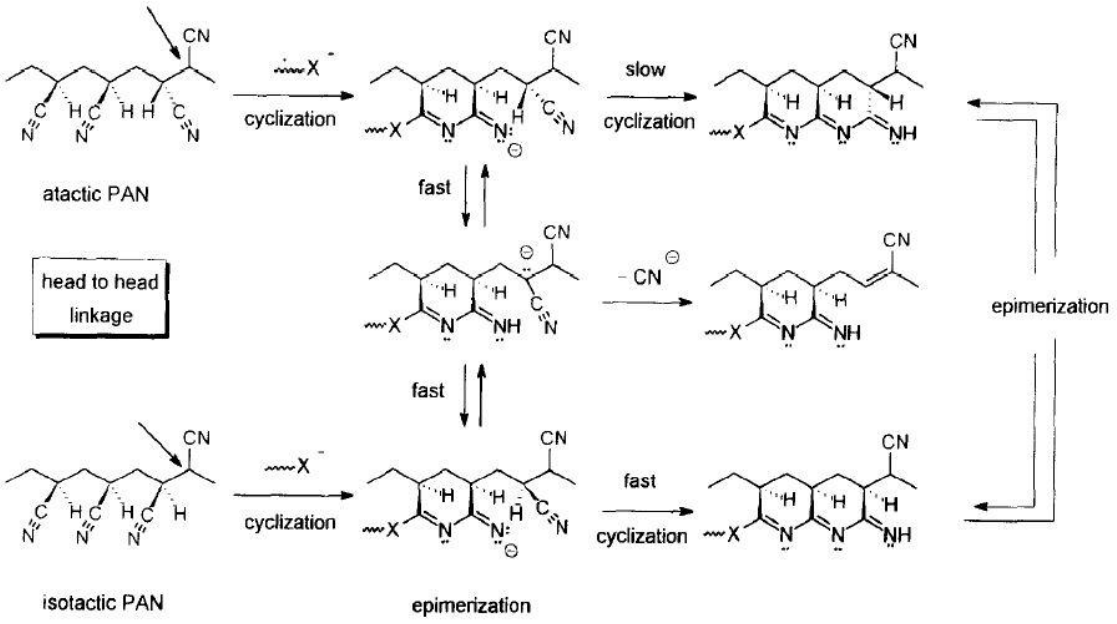

Figure 2: Schematic showing cyclization of PAN [53]

PAN exhibits a phenomenon known as stabilization between the temperature of 200 and 300°C. PAN undergoes a variety of physical and chemical changes owing to several exothermic chemical reactions, including cyclization, dehydrogenation, oxidation, crosslinking and

fragmentation. Cyclization reactions, which convert the linear structure of PAN into an infusible ladder polymer are considered to be most important. [54,60-63]

The cyclization reaction is terminated by the head-to-head linkages with the polymer chain. Ammonia and hydrogen cyanide are released at the same temperature only after the cyclization is complete. At a higher temperature, oligomers are evolved from the uncyclized portion of the polymer.[53]

1.6 PAN/PI blends and copolymers

The stabilization of PAN is a well-known intermediate phenomenon exhibited by PAN to form conjugated ladder structures. Here the effects of PAN content on the thermal and mechanical behavior were systematically investigated to serve as a guide for high-performance polymeric fiber fabrication.

The cyclization of PAA to PI possess an endothermic feature, which can be promoted by the heat released from the cyclization of PAN's nitrile groups. This could potentially accelerate the time-consuming step of stabilization. The high molecular orientation of PI would also affect the orientation of the PAN/PI blend fibers, which lead to the improved mechanical and thermal properties [68]. Alternatively, this composite could also have the potential to produce high-performance carbon fibers since PAN is a useful precursor for carbon fiber production and PI fibers are used for carbonization and graphitization [69,70].

Polyimides (PI) have long been known for their excellent flame resistance with a limited oxygen index (LOI) value of 60. However, they are too expensive to be used in flame retardant applications [71]. Oxidized PAN fibers exhibit similar LOI values ranging between 40-60. Thus, the addition of PAN to PI is focused on reducing the manufacturing cost while retaining the superior flame-retardant properties. Polyimides do not exhibit the property to be drawn into fibers, by adding PAN to form a blend, there is scope for it to be drawn into fibers which could then be used for several applications.

Chapter 2

Experimental

2.1 Materials

The reagents used in this study are as follows: pyromellitic dianhydride anhydride (99% purity), 4, 4'- diamino diphenyl ether (99% purity), 1 -methyl-2-pyrrolidone (99% purity) and the polyacrylonitrile (PAN) with an average molecular weight of 150,000 were purchased from Sigma Aldrich. All the reagents listed above are of analytical grade; AR. De-ionized water was also used in this process.

2.2 Synthesis and Preparation

2.2.1 Synthesis of PAA using condensation method

200ml of NMP is poured into a three-necked flask with a supply of constant dry air, into which 19.046 of ODA was added under continuous stirring for 30 minutes at 10℃. After 5 hours of stirring 20.962gms of PMDA was added into the flask and stirring was continued for another 18hrs after which the mixture was transferred in to glass containers which were purged with nitrogen. The solution is then degassed in a vacuum chamber to remove dissolved air and is then stored in a dry and dark atmosphere.

2.2.2 Preparation of PAN solution

2g of PAN is dissolved in 200ml of NMP at 80℃ with constant stirring. The resulting solution is a 1 wt.% solution of PAN in NMP which is then cooled and stored in a desiccator.

2.2.3 Ex-situ synthesis of PAN/PI blend

The prepared PAN solution is added in measured quantities to yield 0.1, 0.5, 1, 5, 10 wt.% PAN in the PAA. The solutions are then subjected to mechanical stirring and then ultra-sonicated for 30 minutes after which they are stored in a dark and dry atmosphere.

2.2.4 Film Preparation

The PAA/PAN solution along with neat PAA are casted onto a glass substrate in a vacuum oven initially for 60℃ after which the temperature is ramped up to 120℃, 160℃, 200℃ and finally 300℃ for 4 hours each. A stepwise increase in temperature is utilized to prevent cracking due to thermal shock.

2.3 Compositional Analysis

2.3.1 Fourier Transform Infrared Spectroscopy (FT-IR)

Attenuated Total Reflectance FTIR was performed using Nicolet 6700 FT-IR instrument (Smart Orbit ATR accessory with diamond crystal) over a wavelength range of 3500cm^{-1} to 400cm^{-1} to determine the chemical composition and the degree of imidization of the blend.

2.4 Morphology

2.4.1 Optical microscopy

Optical microscope was performed analyse the effect of surface morphology of PI upon the addition of PAN. T690PL Amscope microscope was used to take images at 4x, 10x, 40x and 100x resolutions.

2.5 Mechanical Properties

2.5.1 Dynamic Mechanical Analysis

Dynamic Mechanical Analysis (DMA) was used to determine the viscoelastic properties of the blend films. Samples with dimensions of 20mm x 10mm x 0.06mm in a temperature range of 25℃ to 600℃ were analyzed using EXSTAR 6000, manufactured by Seiko Instruments.

2.6 Thermal properties

2.6.1 Thermogravimetric Analysis (TGA)

TGA was used as a method to empirically assess the thermal stabilities of the polymer blend films. Samples of known weight were heated at a rate of 10℃/min in an inert atmosphere up to temperature of 700℃ to study degradation and char retention.

TGA Q50 953501-301 Thermogravimetric Analyzer (6275) by TA Instruments was used to perform the test.

2.6.2 Differential Scanning Calorimetry (DSC)

DSC was used to assess properties such as thermal stability, heat released and rate of change of enthalpy. Samples of known weight were heated at a rate of 5℃/min in an inert atmosphere up to temperature of 700℃ to measure heat released and enthalpy changes. A heating rate of 30℃/min was used to determine degradation behavior of the blends. EXSTAR6000, Differential Scanning Calorimeter manufactured by Seiko instruments was used to perform the test.

Chapter 3

3.0 Results and Discussion

3.1 Fourier Transform Infrared Spectroscopy

3.1.1 Structural analysis

Imidization is an important aspect for polyimides since it affects the properties of the resultant films. The process of imidization is highly temperature dependent and involves dehydration; the removal of water, which is then followed by cyclization; the closing of the imide ring [72]. The effect of weight fraction of PAN on imidization of PAN/PI blends is studied. Studies have shown that additives alter imidization by increasing the surface area on which it can take place [73]. Figure 3 shows FTIR spectra for PAN/PI blends, neat PI and neat PAN. The absorption bands of Neat PAN and Neat PI are indicated in tables 1 and 2 respectively.

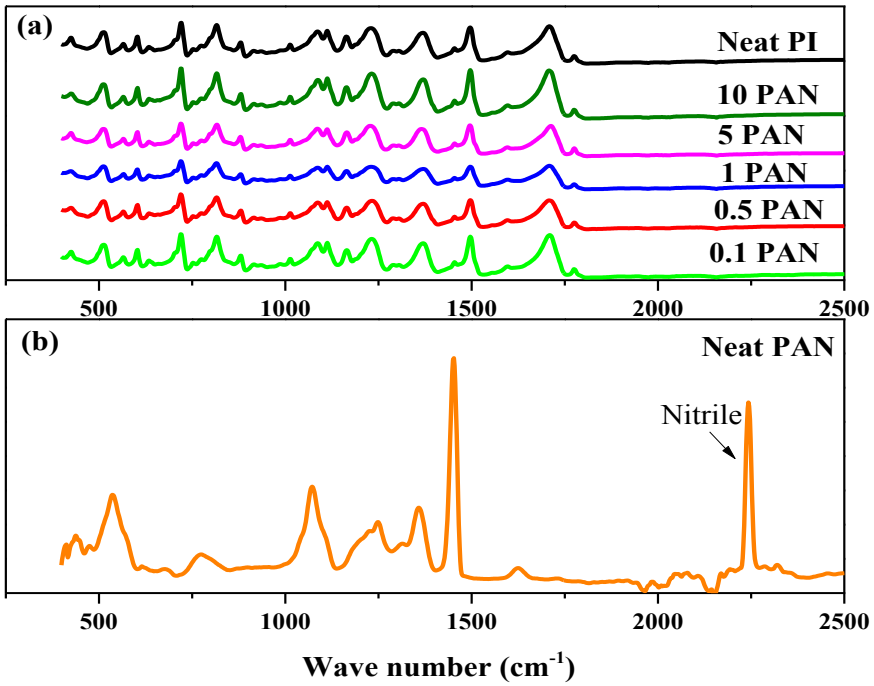

Figure 3: FTIR spectra for (a) Neat PI, PAN/PI blends and (b) Neat PAN

Table 1: Absorption Bands for PAN

Band Position	Band Characterization
2938,1453,1357,1249	Aliphatic Stretching CH, CH_2 and CH_3
2242	C≡N nitrile group
1623	Weak amide group

Table 2: Absorption Bands for PI

Band Position	Band Characterization
3550-3250	N-H stretching
3100-3000	C-H stretching
1778	C=O asymmetric stretching of imide
1716	C=O asymmetric stretching of imide
1647	C=O stretching of amide
1612	C=N/N-H coupled deformation of amide
1543	δ(N-H) of amine
1496	C=C stretching of p-substituted benzene
1408	NMP absorption
1365	C-N-C stretching of imide group
1238	V(C-O-C) between two aromatic rings
1050	C-H in-plane bending
725	Symmetric C=O stretching

PI exhibits characteristic absorption bands at ~1778, 1365 and 1716 cm^{-1} due to asymmetric carboxylic acid stretch, C-N stretch and asymmetric C=O stretching respectively. The peak at 1495 cm^{-1} is associated with stretching of phenyl ring.[74]

PAN exhibits peaks at 2242 cm^{-1} indicating nitrile group, 2938, 1453, 1357 ,1249 cm^{-1} indicating the aliphatic groups (CH, CH_2 and the CH_3 groups) and a weak amide peak at 1623 cm^{-1} is also present [75]. Disappearance of peaks at 2940 and 2240 cm^{-1} is due to cyclization of PAN. New peaks appear at 800 and 1600cm^{-1}, these are due to the formation of C=C, C=N and =C-H bonds [76][77].

3.1.2 Degree of Imidization

DOI is calculated using equation 1. The peaks at 1776 cm^{-1} which represents asymmetrical stretching of C=O ketone bond are normalized with the peak of 1496 cm^{-1} which is indicative of phenyl peak [78][79]. Table 4 shows DOI values of PAN/PI blend.

$$DOI = \frac{\left(A_{1776}/A_{1496}\right)_{Blend}}{\left(A_{1776}/A_{1496}\right)_{Neat}} \times 100 \quad (1)$$

Where A represents area under the respective peaks for blend and neat PI.

In figure 4, peaks 1496 and 1776 cm^{-1} of neat PI and PAN/PI blend are shown. The 1776 cm^{-1} peak represents C=O asymmetrical stretching of polyimide and is observed to move to the right in case of the blend. Due to the presence of nitrile group, which is highly electronegative, the bond length decreases which shifts the peak towards higher wave numbers [80].

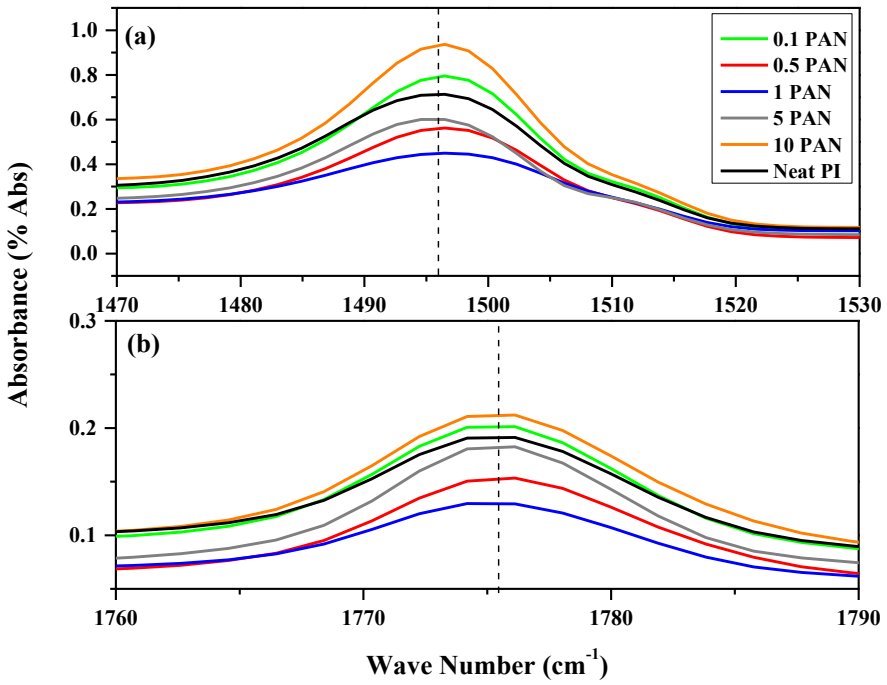

Figure 4: FTIR graphs for neat PI and PAN/PI blends at (a) 1496 cm^{-1} and (b) 1776 cm^{-1} peaks

Table 3: Peak height values for PAN/PI blend compositions at 1776 and 1496 cm^{-1} peaks

Composition (% PAN)	Peak Height	
	1776 cm^{-1}	1496 cm^{-1}
0	0.7	0.19
0.1	0.79	0.2
0.5	0.55	0.15
1	0.44	0.13
5	0.59	0.18
10	0.93	0.21

This shift in peaks however is not exhibited in the phenyl peaks indicating that nitrile group does not affect its development. This phenomenon does not have any effect on degree of imidization as showing in table 4 and figure 5.

Table 4: Degree of Imidization values for PAN/PI blends

Composition (% wt PAN)	A_{1776}	A_{1496}	DOI (%)
0.1	1.89	12.87	95.09
0.5	1.65	11.46	96.93
1	1.11	7.56	94.76
5	1.61	11.05	95.72
10	2.06	14.60	98.68

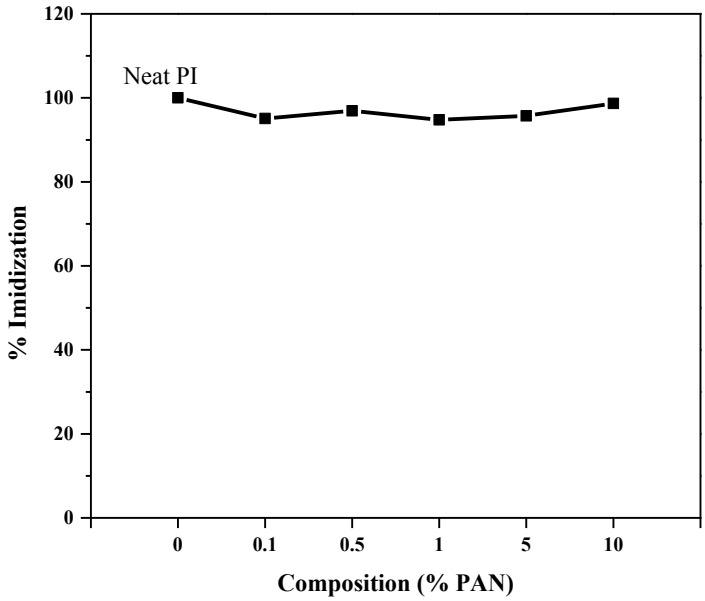

Figure 5: Plot showing degree of Imidization (DOI) vs % composition.

3.2 Optical Microscopy

Figures 6-11 show optical micrographs for neat PI, 0.1, 0.5, 1, 5 and 10% PAN/PI compositions, respectively at different resolutions in color and grey-scale images.

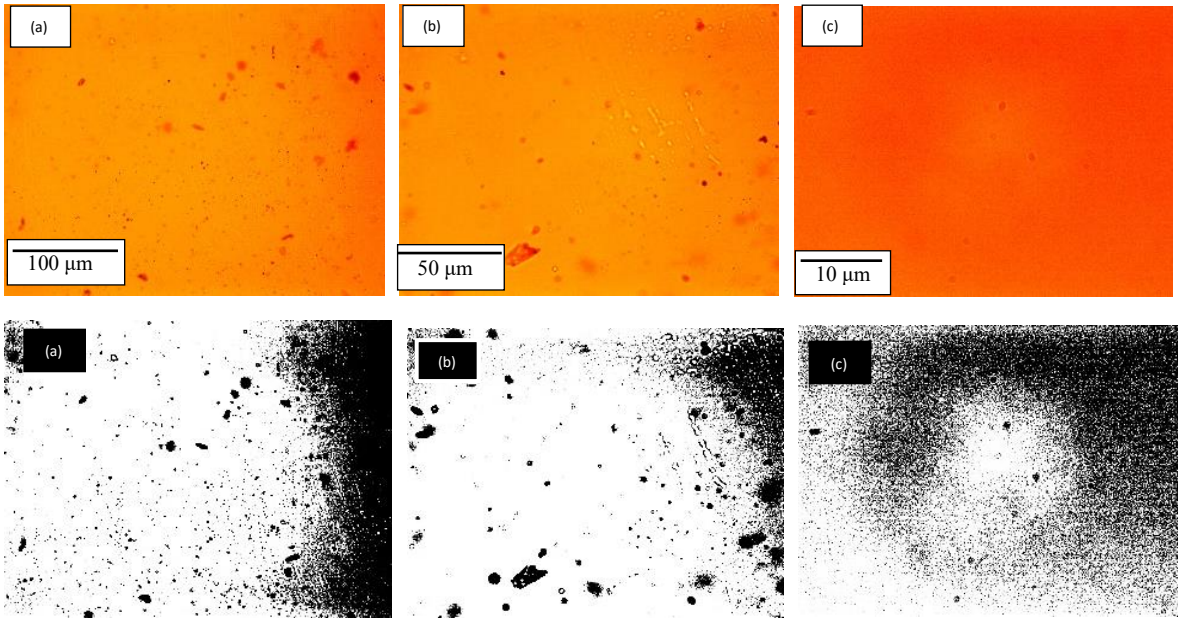

Figure 6: Micrographs of Neat PI

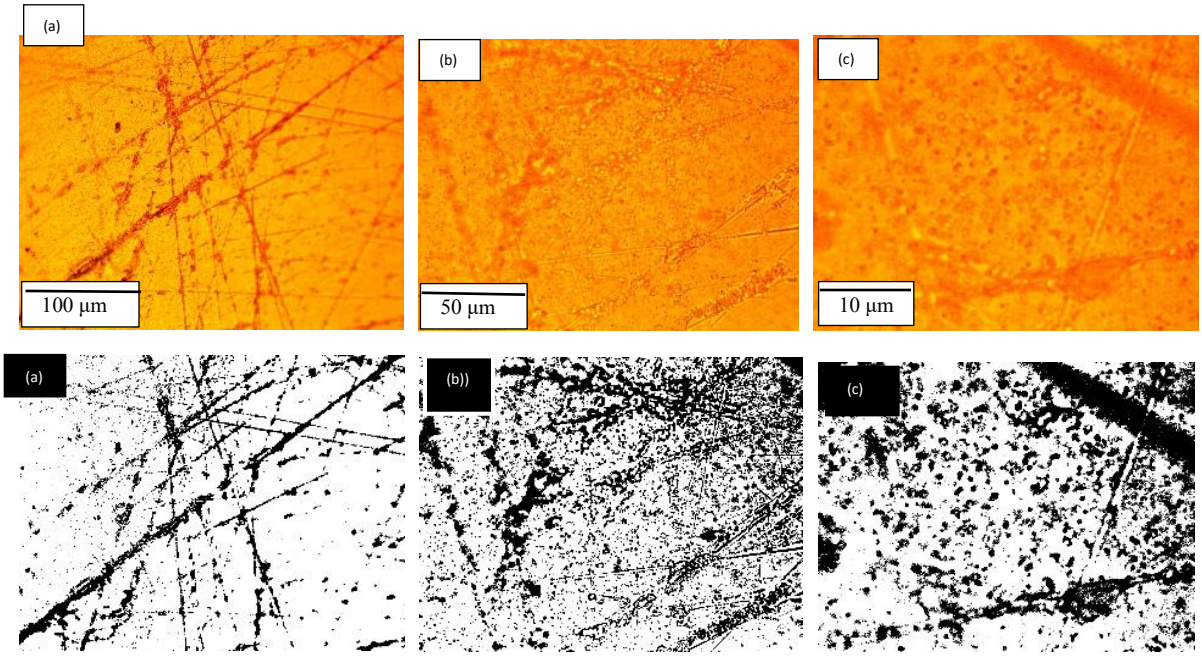

Figure 7: Micrographs of 0.1 PAN/PI

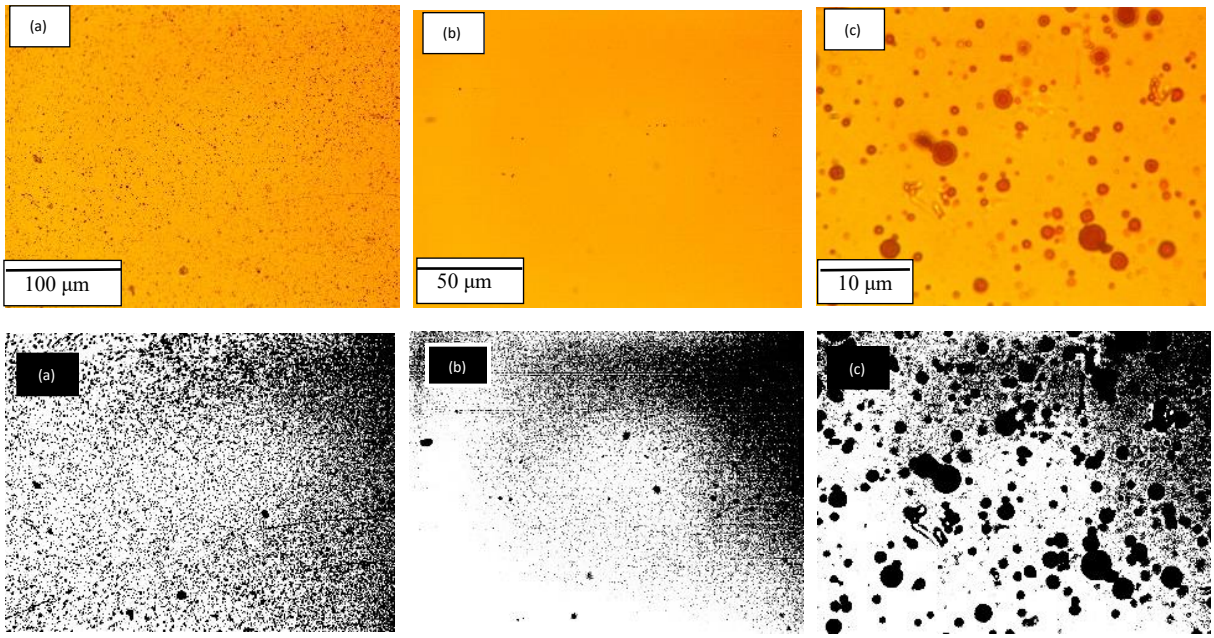

Figure 8: Micrographs of 0.5 PAN/PI

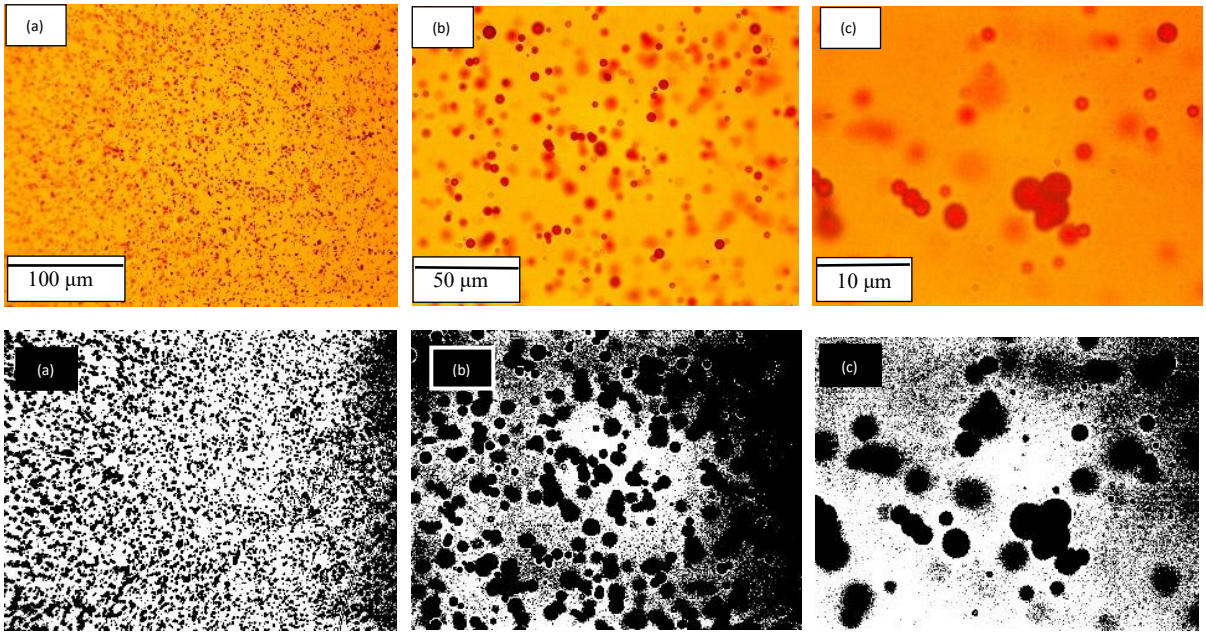

Figure 9: Micrographs of 1 PAN/PI

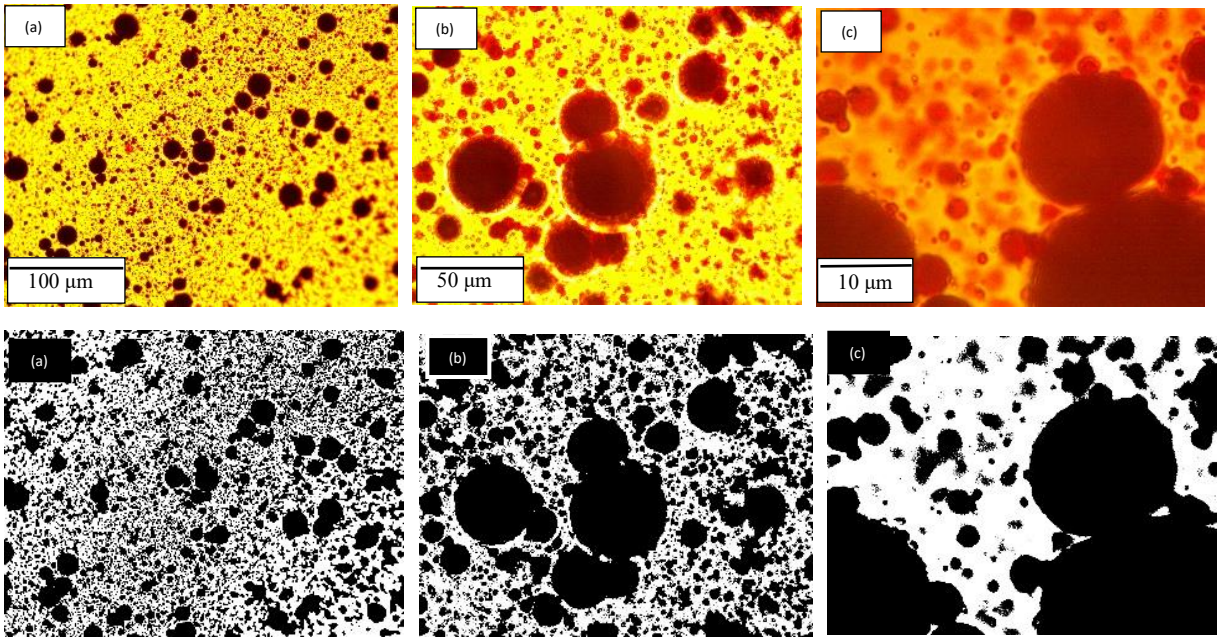

Figure 10: Micrographs of 5 PAN/PI

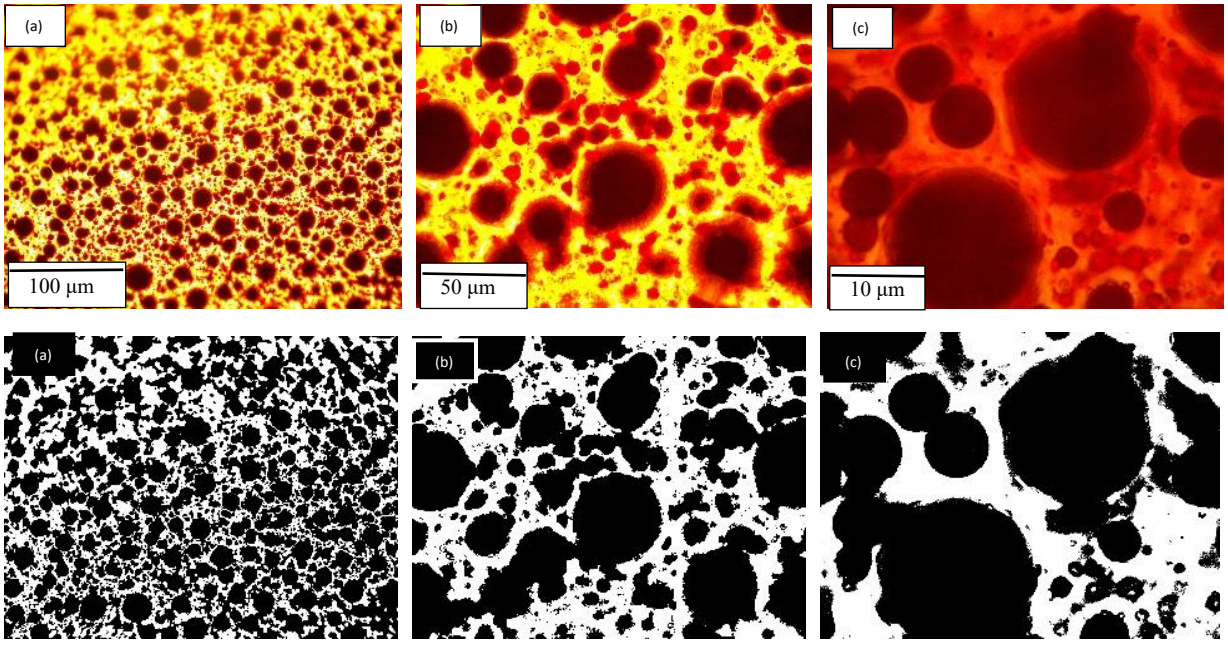

Figure 11 Micrographs of 10 PAN/PI

Optical microscopy was performed to determine the effect of PAN on morphology of PI. Presence of PAN can be observed as dark regions of micrograph. It can be seen that the distribution of PAN particles of varying shapes and sizes is quite uniform within the PI matrix.

With increase in weight fraction of PAN an increase in average particle size is observed. This could be due to the PAN particles coming close to each other as a result of hydrogen bonding and forming globule-like structures [99]. Hence, varying sizes and shapes of PAN particles are observed, especially at higher PAN content.

The presence of large particles of PAN within the PI structure affects the thermo-mechanical properties of the blend. The results from the following experiments will corroborate the findings from optical microscopy.

3.3 Dynamic Mechanical Analysis

Dynamic mechanical analysis provides information on the mechanical properties of polymers undergoing sinusoidal deformation as a function of temperature [81],[87]-[89]. This technique was used to determine the influence of addition of PAN on structural and mechanical properties of PI. Viscoelastic behavior from the glassy region to the rubbery region is studied as a function of temperature. Loss factor (tan δ) vs temperature of neat PI, neat PAN and blends containing 1, 5 and 10% PAN is plotted as shown in figure 12.

3.3.1 Glass Transition Temperature

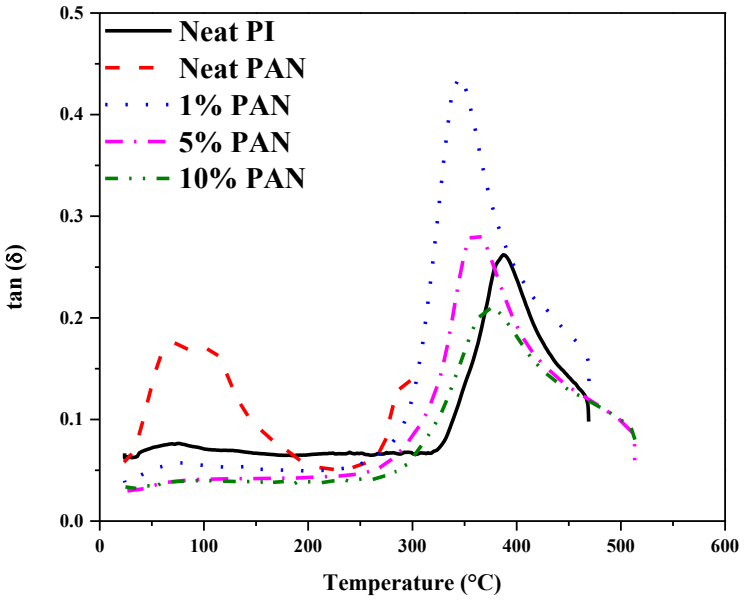

Figure 12: Plot showing Tan delta vs temperature curves for neat PI, neat PAN, 1, 5 and 10% PAN/PI

Tan δ plot was used to determine the glass transition temperature of neat PI, neat PAN and PAN/PI blends. The temperature corresponding to the peak of tan δ curves is considered as the glass transition temperature. From figure 13 it can be observed that neat PI shows a Tg of ~388°C and neat PAN has a Tg of ~89°C. This is corroborated by others [83]-[84]. A corresponding change in the storage modulus is observed in figure 15. The region that occurs before the Tg peak is glassy since a polymer in this region exhibits plastic deformation. As temperature increases there is a change in the slope of the storage modulus indicating glass transition. With further increase in temperature the peak flattens out into a rubbery plateau where

the polymer exhibits elastic deformation [85]. This is followed by flow region where the polymer flows like a liquid. From table 5, it can be observed that addition of PAN results in a decrease in Tg by ~40℃. This could be due to restrictions in chain motion caused by the presence of increased amounts of PAN in PI matrix [86]. Additionally, the tan (δ) peaks for PAN/PI blends exhibit a single Tg peak indicating a good miscibility between the individual components [92].

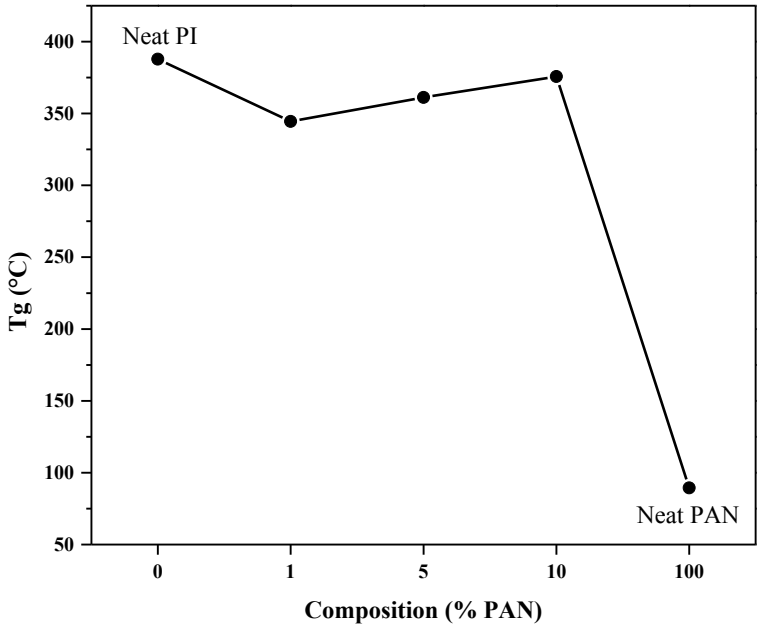

Figure 13: Plot showing variation of Tg with composition.

Table 5: Table showing Tg (°C) and tan (δ) area for all the compositions

Composition (% PAN)	Tg (°C)	Tan(δ) area (a.u.)
Neat PI	~ 388	12.6
1	~ 345	26.7
5	~ 361	18.1
10	~ 376	16.9
Neat PAN	~ 89	11.2

Theoretical Tg for polymer blends can be calculated using Fox equation as shown below [88][89].

$$\frac{1}{Tg} = \frac{W1}{Tg1} + \frac{W2}{Tg2} \quad (2)$$

Where Tg is the glass transition temperature of the blend, W_1 and W_2 are the weight fractions of the individual polymer components and T_{g1} and T_{g2} are the glass transition temperature of the respective polymers. Upon substituting suitable values, a theoretical Tg ranging between 333 – 365 °C is obtained which lies close to the values obtained from testing.

3.3.2 Damping ability

Damping property or the loss factor helps in identifying the nature of molecular motion that exists in the material. The ability of the material to regain its original shape after deformation is revealed by the intensity of the damping peak [81]. Damping ability was determined by measuring the area under the tan (δ) peak for all the compositions (figure 12). Damping ability is dependent on availability of free volume or free movement of polymer chains which is critical for dissipating the absorbed energy. From table 5, it is observed that damping abilities of Neat PI and neat PAN are quite similar as their tan (δ) values are close enough. 1%

PAN/PI composition exhibits the highest damping ability. It is seen that further increase of PAN has decreased damping, this could be attributed to reduced flexibility and higher degrees of interactions within the composite. However, all the PAN/PI blends show an improved damping ability when compared to neat PI. This drop is due to the presence of PAN and its interaction with the PI matrix that is reducing free volume, thus, restricting the energy dissipation [82].

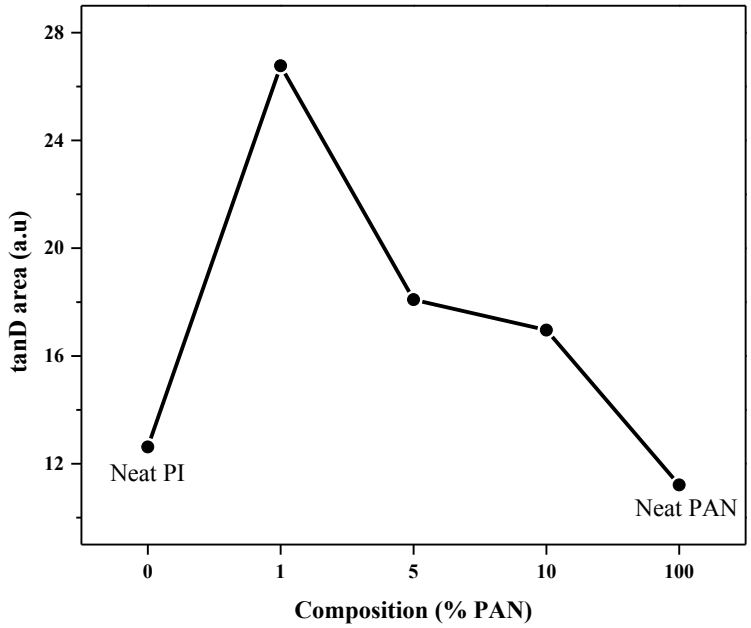

Figure 14: Plot showing tan (δ) vs temperature for neat PI, neat PAN and 1, 5 and 10% PAN/PI

3.3.3 Storage modulus

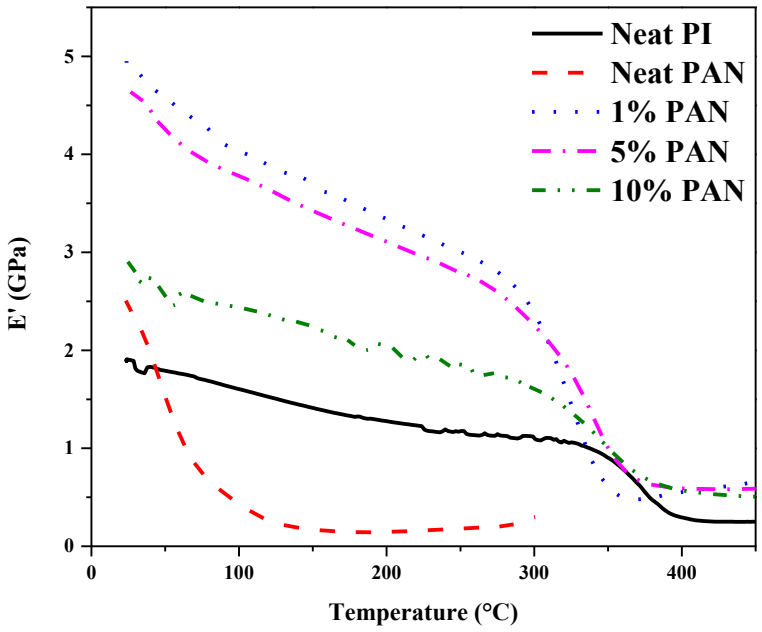

Figure 15: Plot showing storage modulus (GPa) vs temperature for all compositions

Storage modulus plot gives the measure of stiffness of the film when subjected to tensile loading at room temperature [87]. Figure 15 shows variation of storage modulus vs temperature for all the compositions. It was observed that the storage modulus of PAN/PI blend at glassy region (before Tg) is ~2.5 times higher than that of neat PI. Neat PI exhibits the lowest storage modulus at room temperature while the highest modulus is exhibited by 1% PAN/PI. Addition of further PAN results in a decrease in the initial modulus implying increased amount of interactions which reduces the free volume.

As the temperature increases, it is observed that storage modulus of the blend drops at a faster rate than compared to that of neat PI. This implies that the polymer chains have obtained enough energy for long range motion which is nothing but the glass transition temperature.

At temperatures close to 350℃, the storage modulus of the blends begins to drop; this is not seen in neat PI until temperatures close to 390℃. After this region, the storage modulus curve begins to flatten out owing to the interactions which prevents further slippage of the polymer chains. This region is the rubbery plateau at which 10% PAN/PI shows the highest modulus.

The glassy region modulus indicates the rigidity of the material below Tg. It can be seen here that there is a significant increase in glassy region modulus for 5% PAN/PI. The modulus decreases slightly for 10% PAN/PI. This shows that addition of 5% PAN is synergistically reinforcing the blend. The rubbery plateau region modulus was measured at 400℃ for neat PI and the blends and at 200℃ for neat PAN. The appearance of rubbery plateau region indicates entanglements or crosslinks. Both the width and the properties of the region depend on the molecular weight between crosslinks. This is proven by the values of glassy and rubbery region modulus listed in table 6.

Table 6: Glassy region and rubbery region modulus for all the compositions

Composition (%PAN)	**Glassy region modulus (GPa)**	**Rubber plateau modulus (GPa)**
Neat PI	1.90	0.28
1	2.50	0.54
5	4.96	0.59
10	4.63	0.57
Neat PAN	2.92	0.15

3.4 Thermo-Gravimetric Analysis

Thermogravimetric analysis helps in understanding the thermal degradation behavior of the material. The degradation behavior of material when subjected to a controlled increase in temperature is recorded as mass loss percentage [93]. In this study, TGA was performed on cured PAN/PI films with different weight fractions of PAN. The data obtained was used to determine the percentage mass retained and rate of mass loss in neat PI, neat PAN and PAN/PI blend.

3.4.1 Thermal behavior in nitrogen atmosphere

3.4.1.1 Percentage mass retained study

Figures 16 and 17 compare percentage mass retained and derivative mass loss as functions of temperature for neat PI and neat PAN, respectively.

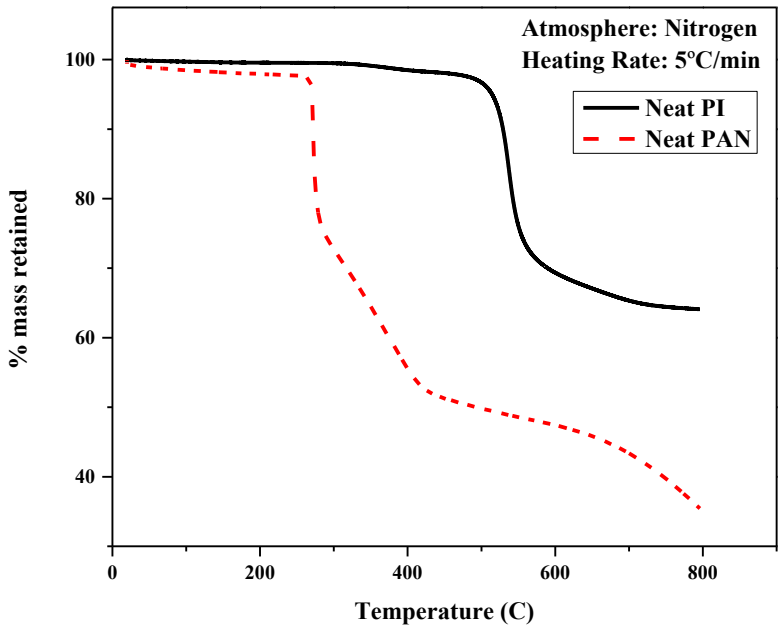

Figure 16: Plot showing % mass retained vs temperature (°C) for neat PAN and neat PI in Nitrogen atmosphere

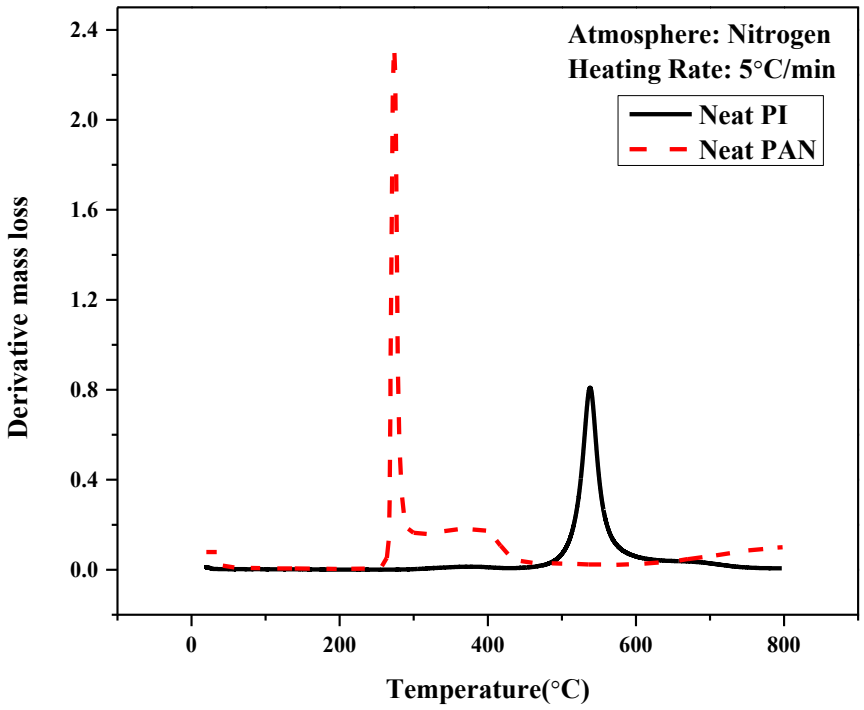

Figure 17: Plot showing derivative mass loss vs temperature (°C) for neat PAN and neat PI in Nitrogen atmosphere

In figure 16, it is seen that both Neat PI and Neat PAN lose mass steadily till 280°C where PAN exhibits a sharp drop implying the onset of degradation. This continues till 300°C where the curve flattens out indicating the cyclization of PAN [94]. This is supported by the derivative mass loss curve in figure 17 where a sharp peak is exhibited by neat PAN at 280°C which is indicative of onset of degradation. The narrow peak is approximately 20°C broad and indicates rapid mass loss. The curve flattens at a temperature of 300°C which indicates the onset of cyclization. At higher temperatures we see that oligomers are evolved from the uncyclized portion of PAN which result in a step transition at 400°C [95].

PI on the other hand starts degrading at a temperature of 480°C and proceeds to lose mass till 550°C resulting in approximately 35% loss in mass [96]. Measures to reduce the rate of mass

loss at this temperature will improve PI's thermal stability. From figure 17 it is observed that the decomposition peak of PI is broader and shorter than PAN, indicating that the reaction doesn't occur as rapidly. The rate of mass loss of neat PI and neat PAN is the same at their respective degradation temperatures as shown in table 7.

Table 7: Comparison of rate of mass loss for neat PI and neat PAN in Nitrogen atmosphere

Sample	Rate of mass loss (s^{-1})
Neat PI at 500℃	0.018
Neat PAN at 280℃	0.018

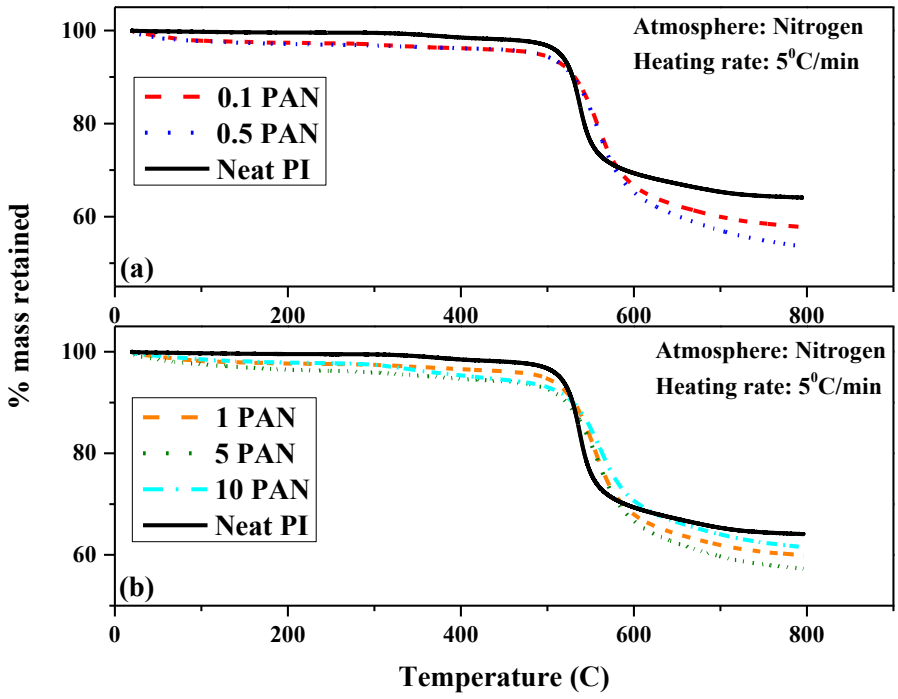

Figure 18: Plot showing % mass retained vs temperature (℃) for (a) Neat PI, 0.1 and 0.5% PAN/PI and (b) Neat PI, 1, 5 and 10% PAN/PI in Nitrogen atmosphere

To compare the effect of addition of PAN to PI the percentage mass retained vs temperature plot for all the compositions is shown in figure 18. It is observed that the addition of PAN results in an initial mass loss. However, the temperature of onset of degradation remains relatively unchanged. The addition of PAN has evidently reduced the slope of the curve which indicates a decrease in the rate of mass loss. It is seen that at higher temperatures (>700℃) both neat PI and PAN/PI blends show similar mass retention.

3.4.1.2 Derivative mass loss study

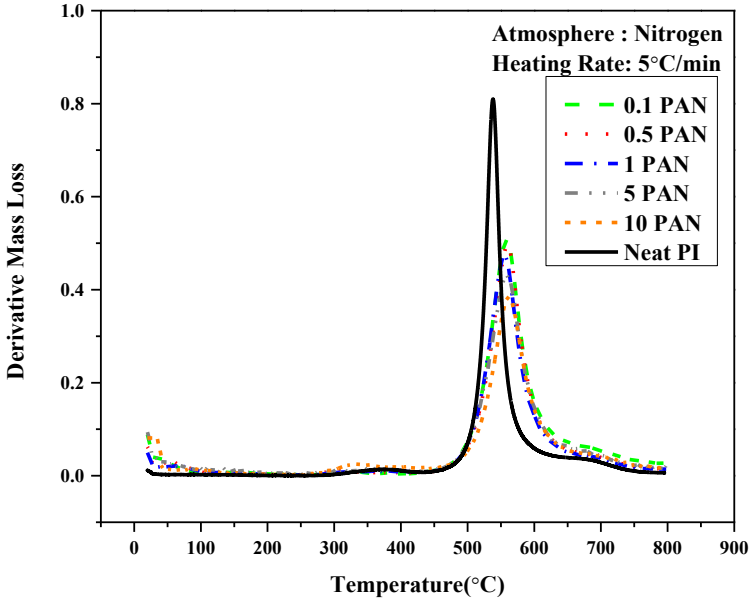

Figure 19: Plot showing derivative mass loss vs temperature (°C) for PAN/PI blends compared to neat PI in Nitrogen atmosphere

From the derivative mass loss curve, it is seen that the addition of PAN has considerably reduced the rate at which the blend degrades. There is a trend that is observed where the increase in PAN added to the blend results in slower rate of decomposition (lower rate of mass loss). Neat PI exhibits the highest rate of mass loss and 10% PAN/PI blend exhibits the lowest (table 8). This phenomenon can be explained by PAN's ability to form a ladder-like structure upon curing at a temperature of 300°C throughout the PI matrix [97]. In case of percentage mass retention of blends, it is seen that increasing weight fraction of PAN results in an increase in mass retained (table 8). As explained by J. Xue et al, the temperature of onset of degradation is where cyclization of PAN occurs and higher mass retention in 10% PAN/PI blend is due to loss in oligomeric PAN influencing the amount of non-volatile residue in the blend [95].

Table 8: Comparison of percentage mass retained for PAN/PI blends in Nitrogen atmosphere

Composition	%Mass Retained
Neat PAN	33.9
Neat PI	64.1
0.1	53.5
0.5	53.5
1	57.3
5	59.9
10	61.3

Table 9: Rate of degradation of PAN/PI blends in Nitrogen atmosphere

Composition (% PAN)	Rate of mass loss (s^{-1})
0.1	0.013
0.5	0.013
1	0.012
5	0.012
10	0.010

Upon comparing the rate of mass loss values of neat PI, neat PAN and PAN/PI blends in tables (7) and (9), there is a trend of decreasing rate of mass loss as shown in figure 20.

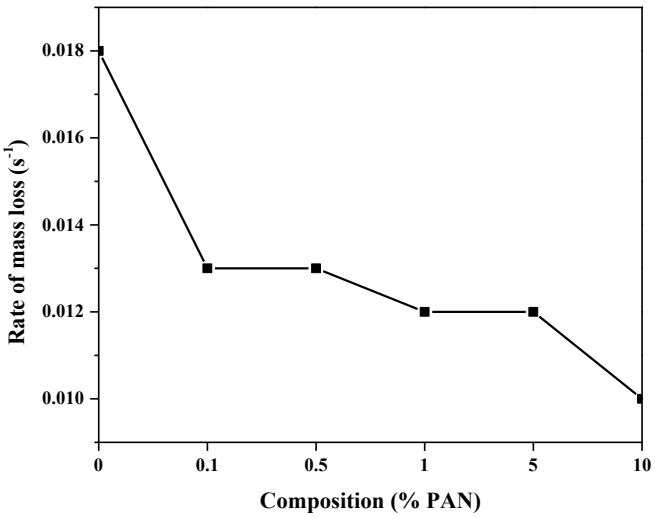

Figure 20: Comparison of rate of mass loss of the blends in Nitrogen atmosphere

3.4.2 Thermal behavior in air atmosphere

3.4.2.1 Percentage mass retained study

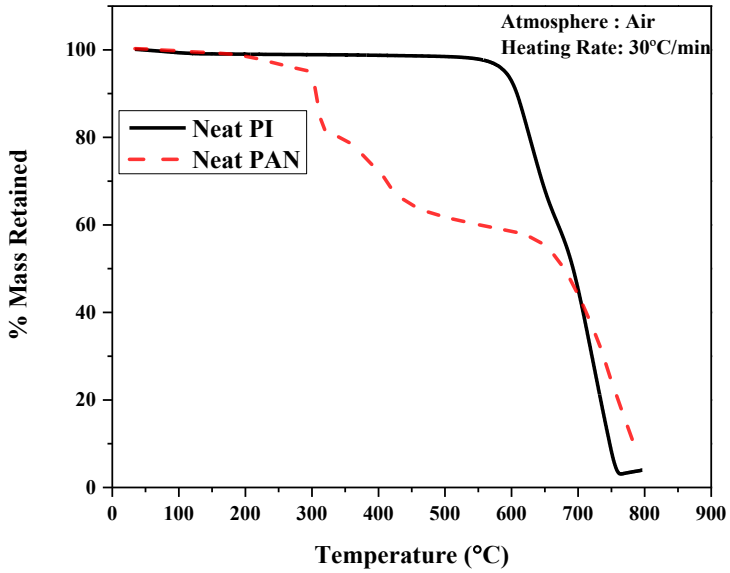

Figure 21: Plot showing % mass retained vs temperature (°C) for Neat PAN and Neat PI in air atmosphere

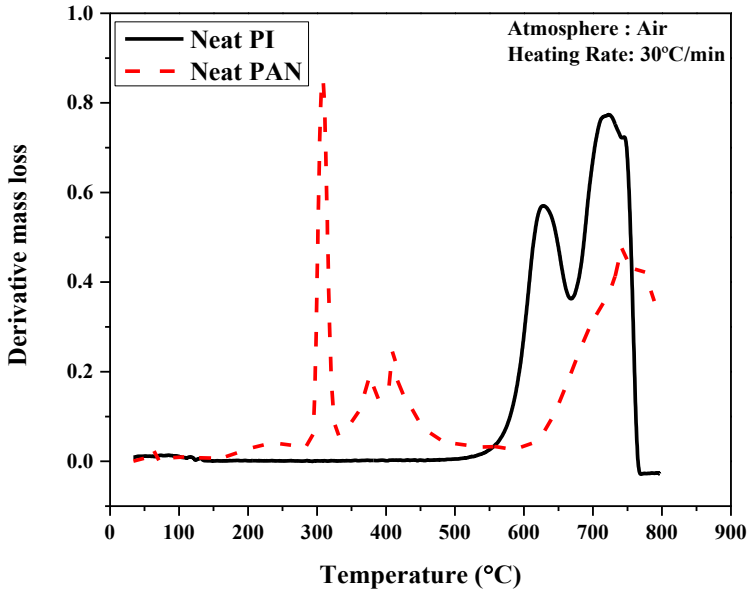

Figure 22: Plot showing derivative mass loss vs temperature (°C) for Neat PAN and Neat PI in air atmosphere

Percentage mass retained and derivative mass loss curves for neat PI and neat PAN are shown in figures 21 and 22, respectively.

Thermal behavior of PAN/PI blend varies according to the atmosphere. While both nitrogen and air show similar properties till temperatures of 600℃, the properties vary after that due to char degradation in air. The char primarily consisting of carbon reacts with the oxygen at higher temperatures and is released in the form of CO and CO_2 gases. Neat PI loses very little mass till ~580℃. This minimal loss of mass can be attributed to un-evaporated solvent and water vapor from the curing process. After crossing the 580℃ however, PI degrades into char. Char provides a certain amount of thermal stability by prevent newer material from getting oxidized.

It can be seen that at temperature close to 670℃, the char begins to decompose. While the degradation peaks are not clearly visible in figure 21, they appear as distinct peaks in figure 22. PAN's decomposition in air shows similar behavior to that of nitrogen atmosphere till the formation of char at temperatures close to 640℃ after which it decomposes to leave behind close to 10% of the original mass. The rate of mass loss of both polymer and char for neat PI and neat PAN is shown in tables 10 and 11.

Table 10: Rate of mass loss of polymer

Composition (%PAN)	**Rate of mass loss (s^{-1})**
Neat PI	0.086
Neat PAN	0.155

Table 11: Rate of mass loss of char

Composition (%PAN)	Rate of mass loss (s^{-1})
Neat PI	0.204
Neat PAN	0.048

To measure the general effect of addition of PAN to PI, a mass retained plot of PAN/PI and neat PI vs temperature is shown in figure 23.

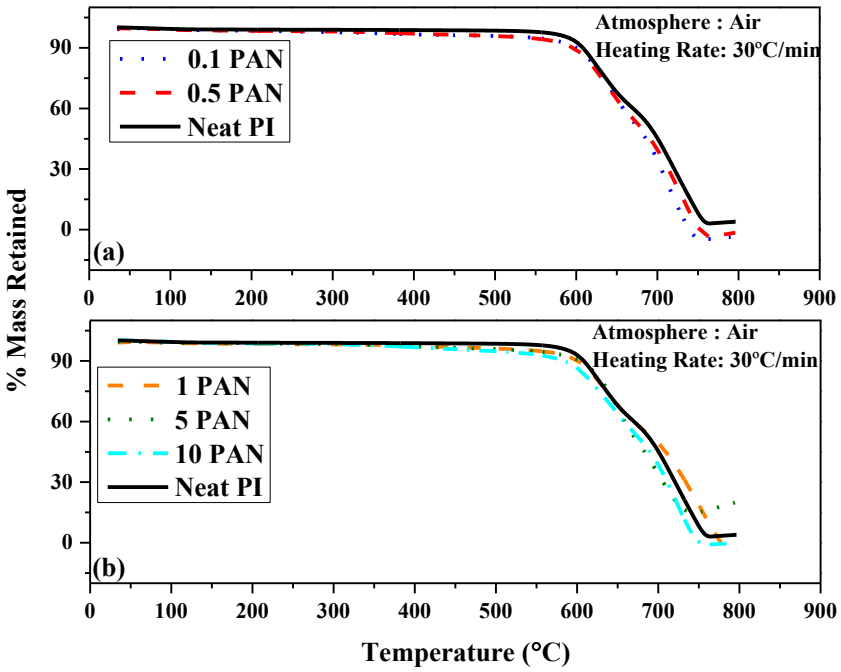

Figure 23: Plot showing % mass retained vs temperature (°C) for (a) Neat PI, 0.1 and 0.5% PAN/PI and (b) Neat PI, 1, 5 and 10% PAN/PI in air atmosphere

Unlike in nitrogen, it observed that due to oxidation of both polymer and char, onset temperatures of the blend is lower than that of neat PI. This effect is less pronounced in the compositions that have lower weight fractions of PAN. From the derivative mass loss curve

shown in figure 24, it can be seen that all samples including neat PI and PAN/PI blends exhibit two peaks after onset of degradation. The first peak area gives the rate of polymer degradation while the second peak area gives rate of char degradation.

3.4.2.2 Derivative mass loss study

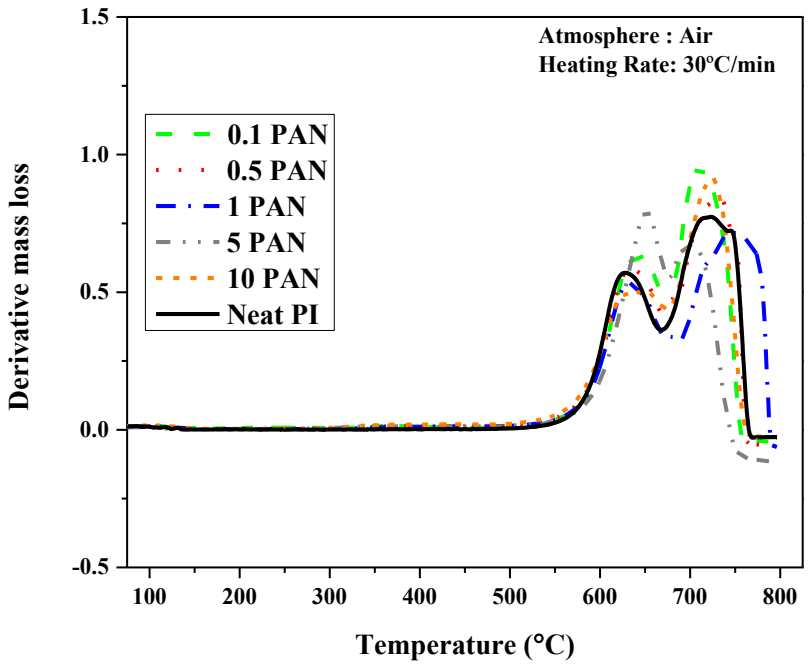

Figure 24: Plot showing derivative mass loss vs temperature (°C) for Neat PI and PAN/PI blends in air atmosphere

The rate of mass loss of polymers and their char are shown in tables 12 and 13, respectively. It can be observed that addition of PAN has increased the onset of degradation for both the polymer and the char in all the samples. This can be attributed to the stabilization of PAN which is improving blend's thermal stability. Research by Xiao et Al [98] shows that PAN stabilizes to a higher degree in the presence of oxygen due to formation of conjugated C=O structures which

facilitate in further dehydration and increase the interactions with the PI matrix which could be reinforcing the blend.

Table 12: Rate of degradation of PAN/PI blend polymers in air

Composition (%PAN)	Onset of Degradation (°C)	Rate of mass loss (s^{-1})
Neat PI	522.66	0.084
0.1	534.57	0.069
0.5	537.59	0.073
1	530.79	0.077
5	539.67	0.078
10	536.84	0.058

Table 13: Rate of degradation of char in air

Composition (%PAN)	Onset of Degradation (°C)	Rate of mass loss (s^{-1})
Neat PI	666.9	0.203
0.1	676.73	0.215
0.5	685.62	0.228
1	690.15	0.206
5	677.49	0.284
10	675.22	0.199

Through the rate of degradation of the polymer and the char, it can be observed that PI containing 10% PAN shows the slowest rate of mass loss. This could imply a direct correlation between increased interaction of stabilized PAN improving thermal stability. The rate of mass loss values of both polymers and their char as plotted against composition and are shown in Figure 25.

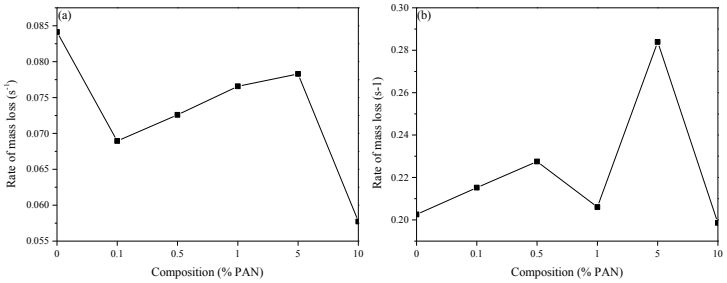

Figure 25: Rate of degradation of PAN/PI blend (a) polymers and (b) char in presence of air

3.5 Differential Scanning Calorimetry

3.5.1 Heat Loss and Change of Enthalpy

Differential scanning calorimetry measures difference in heat flow between a sample and an inert reference as a function of time and temperature where both the sample and the inert reference are subjected to a controlled environment [96]. The change in heat flow occurs when there is a transition in the sample. The heat flow is then plotted on y-axis against temperature on the x-axis.

In this study, DSC was performed on cured PAN/PI films with different weight fractions of PAN. Data obtained was used to determine the transitions occurring in the blend during the heating cycle. The obtained data is then compared to the thermal behavior of both neat PI and neat PAN. Figure 26(a) shows the thermograms of PAN/PI in comparison with neat PI. Figure 26(b) compares thermograms of neat PI and neat PAN.

Neat PAA exhibits an endothermic behavior during imidization, this dip in the curve is missing in the neat PI indicating complete imidization, corroborated by FTIR spectra table 4. In neat PAN's thermogram a sharp and narrow peak indicates a rapid reaction, which in PAN's case implies stabilization [97]

From figures 26a and 26b, it can be stated that the addition of PAN has a definite effect on thermal behavior of PI. In case of neat PAN, the peak found at 280°C is absent indicating complete stabilization during the cure. PAN cyclizes at temperature of ~280°C and forms a network like structure in the matrix of PI. In the thermograms of PAN/PI blends, it is observed that peaks ~600°C broaden implying improvement in thermal properties (reduction in heat released) over that of neat PI. Area under the peaks is measured to calculate enthalpy which is then divided by time between the peak to give rate of change of enthalpy. This value is then divided with the weight of the initial sample that gives us the rate of heat released upon degradation. The values are shown in table 14.

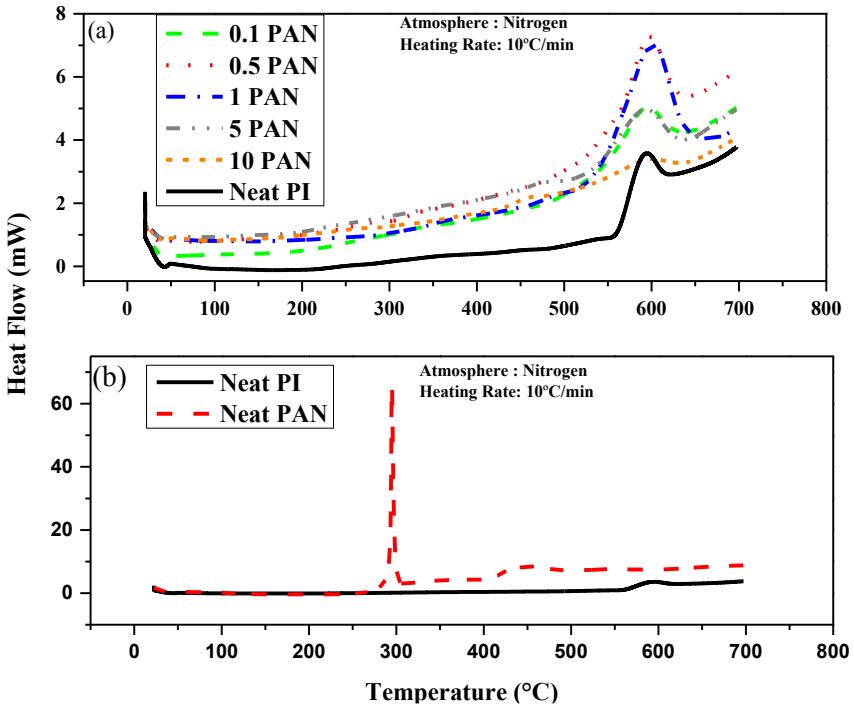

Figure 26: DSC thermograms for (a) PAN/PI blends and neat PI, and (b) neat PAN and neat PI in Nitrogen atmosphere.

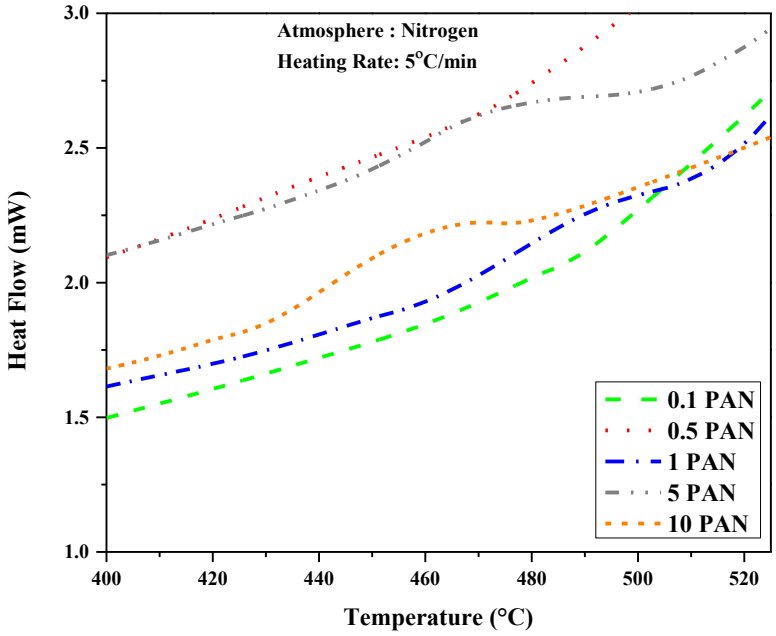

Figure 27: DSC thermograms of PAN/PI blends between 400ºC and 525ºC in Nitrogen atmosphere

From figure 27, it can be seen that higher weight fractions of PAN (>1%PAN) exhibit a step at temperatures between 450°C and 500°C. This peak is also seen in neat PAN where the oligomers release by the uncyclized PAN begin to degrade (figure 25). It is seen that increasing the weight fraction of PAN moves the step towards left indicating higher PAN weight fraction blend exhibit degradation behavior like neat PAN in this temperature range. This phenomenon is not exhibited by neat PI or the lower weight fraction PAN/PI blends.

Table 14: Rate of change of enthalpy of PAN/PI blend.

Composition (wt% PAN)	**ΔH(J)**	**Rate of heat release(J/sec)**
Neat PI	49.63	0.125
0.1	76.52	0.095
0.5	121.1	0.128
1	224	0.124
5	77.81	0.115
10	21.79	0.019

From table 10, it is seen that there is a general trend indicating a decrease in the amount of heat released with increase in weight fraction of PAN.

3.4.2 Degradation Study

For determining thermal degradation behavior of the blends, DSC was performed in air atmosphere at a high heating rate of 30°C/min. A high heating rate is used to simulate conditions of combustion. The thermograms of the blends and neat PI can be seen in figure 28. Samples showing similar thermal behaviors are shown together in figures 29a and 29b.

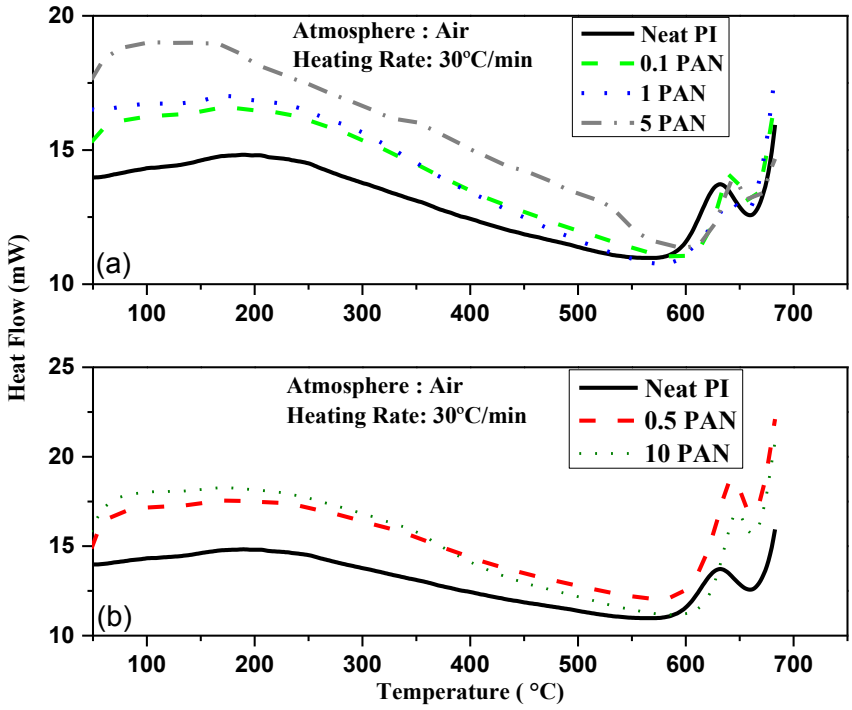

Figure 28: DSC thermograms in air for neat PI and PAN/PI blends containing (a) 0.1, 1 and 5% PAN (b) 0.5 and 10% PAN

The temperature of onset of degradation for both nitrogen and air thermograms is listed in table 15. Blends subjected to heating in air show an increase in their onset temperatures. An interesting observation that can be made by comparing onset temperatures is that while the addition of PAN has reduced the onset temperature in nitrogen atmosphere, the blends exhibit an increased onset temperature implying that the blends show improved thermal properties in conditions where it is exposed to a reactive atmosphere and higher rate of heat. This behavior is explained by Xiao et Al [101] who state that PAN stabilizes better in the presence of oxygen. This could enable the use of PAN/PI blends in application which require thermal stability at higher temperatures.

Table 15: Comparison of onset of degradation temperatures of blend in Nitrogen and air atmospheres

Composition (% PAN)	Temperature of Onset of Degradation(°C)	
	Nitrogen	Air
Neat PI	555.30	576.44
0.1	496.59	600.44
0.5	513.98	584.04
1	518.11	586.04
5	511.31	608.57
10	481.86	600.84

The rate of degradation of films and heat released during degradation are calculated from the DSC thermograms. Enthalpy calculations are made by measuring the area under the peaks. Heat release is calculated by multiplying the change of enthalpy value with mass of the sample. The heat released per second is calculated by dividing the above value with the time of decomposition. The thermal behaviors of the blend can be seen in the graphs shown in figure 29.

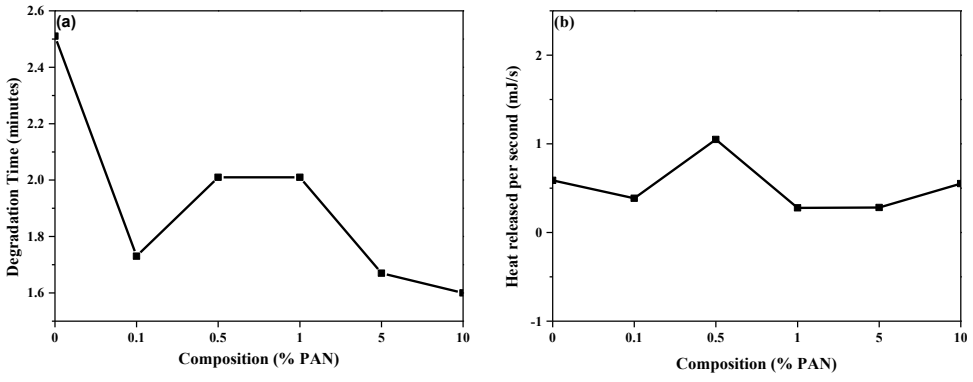

Figure 29: Graphs showing (a) Degradation time vs composition (b) Rate of heat release vs composition.

There is a general trend observed which shows that blends containing higher weight percentage of PAN have lower degradation times. It can also be seen that the rate of heat release of certain blends is comparable with that of neat PI. Table 16 shows the change of enthalpy values and heat release rate corresponding to the blend.

Table 16: Change in enthalpy and rate of heat released of neat PI and PAN/PI blends.

Composition (% PAN)	**ΔH(J)**	**Heat Released per second (J/sec)**
Neat PI	59.05	0.59
0.1	40.21	0.39
0.5	84.45	1.05
1	20.89	0.28
5	28.40	0.28
10	53.23	0.55

4 Conclusion

FTIR was performed on PAN/PI blends to study the effect of addition of PAN on imidization. Higher degree of imidization is indicative of improved mechanical properties such as higher tensile modulus and wear resistance, thermal properties, and chemical properties such as solvent resistance, solvent entrance and impermeability to gas flow. Upon studying the DOI values of PAN/PI blends, it is observed that addition of PAN has interfered minimally with imidization. It is seen that there is a generally positive trend of increasing DOI that is observed with increasing weight fraction of PAN. The film containing 10% PAN shows a 98.6% imidization which is highest amongst all the blend compositions. This could be attributed to the PAN network providing additional surface area and sites for dehydration and cyclization.

From TGA it can be concluded that the addition of PAN has resulted in an increase in the temperature of onset of degradation. It is shown that there is a slight decrease in the mass retained after the heating cycle indicating that the char retention of the blend has reduced. However, upon closely examining the decomposition behavior it is seen that the rate of decomposition is greatly reduced upon the addition of PAN to the PI. This could be because of the cyclization (stabilization) behavior of PAN interfering with the decomposition mechanism. From the thermograms it can be stated that the addition of PAN to PI does not adversely affect the thermal stability of PI, in fact it reduces the rate at which mass is lost by 45%. The addition of PAN to PI results in the formation of a network like structure of stabilized PAN throughout the matrix of PI. The reduced rate of mass loss could be attributed to this structure decomposing before the matrix does thus improving its thermal stability.

From DSC it can be observed that the thermal properties of PAN have been altered. The cyclization behavior exhibited by the neat PAN which resulted in a sharp peak is no longer

present, indicating complete cyclization of PAN during the cure. Also, the secondary peak of the oligomers of PAN is also absent in the blend. Addition of PAN in general broadens the peak implying that the speed at which the blend degrades has reduced. Among all the blend compositions, 10% PAN releases the lowest amount of heat per gram upon degradation implying that the increase in the cyclized PAN network has cause the thermal stability of the blend to improve. PAN/PI blends show an increased temperature of onset of degradation when compared to neat PI.

From DMA it is observed that addition of PAN to PI does not alter the glass transition temperature significantly. The damping ability is found to improve with increasing weight fraction of PAN as compared to neat PI. 5% PAN/PI composition shows synergistic reinforcement at glassy region storage modulus while 10% PAN/PI blend shows the highest rubbery region modulus due to entanglement or crosslinking. Overall it can be said that adding PAN to PI enhances its thermomechanical properties.

4.1 Scope for future work

i) Ability of PAN/PI blend to be drawn into fibers

ii) Synthesis of high-performance carbon fiber using PAN/PI blend

iii) Flammability study

iv) PAN/PI as host material for organo-clay nanocomposites

References

1. Takekoshi, T. (1996). Synthesis of polyimides. Plastics engineering-new york-, 36, 7-48.
2. Ba, C., and Economy, J. (2010). Journal of Membrane Science, 363(1-2), 140-148.Tong, Y., Huang, W., Luo, J., and Ding, M. (1999).
3. Tong, Y., Huang, W., Luo, J., and Ding, M. (1999).
4. Li, Q., Yang, X., Chen, W., Yi, C., and Xu, Z. (2008, January).
5. Jou, J. H., and Huang, P. T. (1991). Effect of thermal curing on the structures and properties of aromatic polyimide films. Macromolecules, 24(13), 3796-3803.
6. Li, W. S., Shen, Z. X., Zheng, J. Z., and Tang, S. H. (1998).
7. Kotera, M., Nishino, T., and Nakamae, K. (2000).
8. Gattiglia, E., and Russell, T. P. (1989).
9. Agag, T., Koga, T., and Takeichi, T. (2001)
10. Ahmad, Z., and Mark, J. E. (2001). Polyimide− ceramic hybrid composites by the sol− gel route. Chemistry of Materials, 13(10), 3320-3330.
11. Yang, J., Zhang, Z., Friedrich, K., and Schlarb, A. K. (2007). Resistance to time-dependent deformation of nanoparticle/polymer composites. Applied physics letters, 91(1), 011901.
12. Burnside, S. D., and Giannelis, E. P. (1995). Synthesis and properties of new poly (dimethylsiloxane) nanocomposites. Chemistry of materials, 7(9), 1597-1600.
13. Vaia, R. A., Vasudevan, S., Krawiec, W., Scanlon, L. G., and Giannelis, E. P. (1995). New polymer electrolyte nanocomposites: Melt intercalation of poly (ethylene oxide) in mica-type silicates. Advanced Materials, 7(2), 154-156.

14. Peng, H., and Sun, X. (2009). Highly aligned carbon nanotube/polymer composites with much improved electrical conductivities. Chemical Physics Letters, 471(1-3), 103-105.
15. Grossiord, N., Loos, J., Van Laake, L., Maugey, M., Zakri, C., Koning, C. E., and Hart, A. J. (2008). High-Conductivity Polymer Nanocomposites Obtained by Tailoring the Characteristics of Carbon Nanotube Fillers. Advanced Functional Materials, 18(20), 3226-3234.
16. Zhu, Z. H. (2015). Piezoresistive Strain Sensors Based on Carbon Nanotube Networks: Contemporary approaches related to electrical conductivity. IEEE nanotechnology magazine, 9(2), 11-23.
17. Aguilar, J. O., Bautista-Quijano, J. R., and Avilés, F. (2010). Influence of carbon nanotube clustering on the electrical conductivity of polymer composite films. Express Polym. Lett, 4(5), 292-299.
18. Kumar, G. A., Chen, C. W., Riman, R., Chen, S., Smith, D., and Ballato, J. (2005). Optical properties of a transparent CaF 2: Er 3+ fluoropolymer nanocomposite. Applied Physics Letters, 86(24), 241105.
19. Gangopadhyay, R., and De, A. (2000). Conducting polymer nanocomposites: a brief overview. Chemistry of materials, 12(3), 608-622.
20. Baibarac, M., and Gómez-Romero, P. (2006). Nanocomposites based on conducting polymers and carbon nanotubes: from fancy materials to functional applications. Journal of nanoscience and nanotechnology, 6(2), 289-302.
21. Zhang, R., Moon, K. S., Lin, W., and Wong, C. P. (2010). Preparation of highly conductive polymer nanocomposites by low temperature sintering of silver nanoparticles. Journal of Materials Chemistry, 20(10), 2018-2023.

22. Gilman, J. W. (1997). Nanocomposites: a revolutionary new flame-retardant approach. SAMPE J., 33, 40.
23. Gilman, J. W. (1999). Flammability and thermal stability studies of polymer layered silicate (clay) nanocomposites. Applied clay science, 15(1-2), 31-49.
24. Bourbigot, S., Bras, M. L., Dabrowski, F., Gilman, J. W., and Kashiwagi, T. (2000).
25. Gilman, J. W., Jackson, C. L., Morgan, A. B., Harris, R., Manias, E., Giannelis, E. P., ... and Phillips, S. H. (2000). Flammability properties of polymer− layered-silicate nanocomposites. Polypropylene and polystyrene nanocomposites. Chemistry of materials, 12(7), 1866-1873.
26. Gusev, A. A., and Lusti, H. R. (2001). Rational design of nanocomposites for barrier applications. Advanced Materials, 13(21), 1641-1643.
27. Nam, S. Y., Park, J. S., Rhim, J. W., Chung, Y. S., and Lee, Y. M. (2006). Gas permeable properties of elastomer-clay nanocomposite membrane. Membrane Journal, 16(2), 144-152.
28. Messersmith, P. B., and Giannelis, E. P. (1995). Synthesis and barrier properties of poly (ε-caprolactone) -layered silicate nanocomposites. Journal of Polymer Science Part A: Polymer Chemistry, 33(7), 1047-1057.
29. Yano, K., Usuki, A., Okada, A., Kurauchi, T., and Kamigaito, O. (1993). Synthesis and properties of polyimide–clay hybrid. Journal of Polymer Science Part A: Polymer Chemistry, 31(10), 2493-2498.
30. Kojima, Y., Usuki, A., Kawasumi, M., Okada, A., Kurauchi, T., and Kamigaito, O. (1993). Synthesis of nylon 6–clay hybrid by montmorillonite intercalated with ϵ-caprolactam. Journal of Polymer Science Part A: Polymer Chemistry, 31(4), 983-986.

31. Giannelis, E. P. (1996). Polymer layered silicate nanocomposites. Advanced materials, 8(1), 29-35.
32. Giannelis, E. P., Krishnamoorti, R., and Manias, E. (1999). Polymer-silicate nanocomposites: model systems for confined polymers and polymer brushes. In Polymers in confined environments (pp. 107-147). Springer, Berlin, Heidelberg.
33. LeBaron, P. C., Wang, Z., and Pinnavaia, T. J. (1999). Polymer-layered silicate nanocomposites: an overview. Applied clay science, 15(1-2), 11-29.
34. Vaia, R. A., Price, G., Ruth, P. N., Nguyen, H. T., and Lichtenhan, J. (1999). Polymer/layered silicate nanocomposites as high performance ablative materials. Applied Clay Science, 15(1-2), 67-92.
35. Sinha Ray, S., and Biswas, M. (2001). Recent progress in preparation and evaluation of montmorillonite/polymer nanocomposites. Adv Polym Sci, 155, 167-221.
36. Huang, J. C., Zhu, Z. K., Yin, J., Qian, X. F., and Sun, Y. Y. (2001). Poly (etherimide)/montmorillonite nanocomposites prepared by melt intercalation: morphology, solvent resistance properties and thermal properties. Polymer, 42(3), 873-877.
37. Tyan, H. L., Leu, C. M., and Wei, K. H. (2001). Effect of reactivity of organics-modified montmorillonite on the thermal and mechanical properties of montmorillonite/polyimide nanocomposites. Chemistry of materials, 13(1), 222-226.
38. Morgan, A. B., Harris Jr, R. H., Kashiwagi, T., Chyall, L. J., and Gilman, J. W. (2002). Flammability of polystyrene layered silicate (clay) nanocomposites: carbonaceous char formation. Fire and Materials, 26(6), 247-253.
39. Agag, T., and Takeichi, T. (1999).

40. Gu, A., Kuo, S. W., and Chang, F. C. (2001). Synthesis and properties of PI/clay organoclays. J. Appl. Polym. Sci, 79, 1902-1910.
41. Kim, J. S., Lee, M. J., Kang, M. S., Yoo, K. P., Kwon, K. H., Singh, V. R., and Min, N. K. (2009). Fabrication of high-speed polyimide-based humidity sensor using anisotropic and isotropic etching with ICP. Thin Solid Films, 517(14), 3879-3882.
42. Giannelis, E. P., Krishnamoorti, R., and Manias, E. (1999). Polymer-silicate nanocomposites: model systems for confined polymers and polymer brushes. In Polymers in confined environments (pp. 107-147). Springer, Berlin, Heidelberg.
43. Yeh, J. M., Chen, C. L., Chen, Y. C., Ma, C. Y., Lee, K. R., Wei, Y., and Li, S. (2002). Enhancement of corrosion protection effect of poly (o-ethoxyaniline) via the formation of poly (o-ethoxyaniline)–clay nanocomposite materials. Polymer, 43(9), 2729-2736.
44. Messersmith, P. B., and Giannelis, E. P. (1995). Synthesis and barrier properties of poly (ε-caprolactone) -layered silicate nanocomposites. Journal of Polymer Science Part A: Polymer Chemistry, 33(7), 1047-1057.
45. Kornmann, X., Lindberg, H., and Berglund, L. A. (2001). Synthesis of epoxy–clay nanocomposites: influence of the nature of the clay on structure. Polymer, 42(4), 1303-1310.
46. Wang, M. S., and Pinnavaia, T. J. (1994). Clay-polymer nanocomposites formed from acidic derivatives of montmorillonite and an epoxy resin. Chemistry of Materials, 6(4), 468-474.
47. Kelly, P., Akelah, A., Qutubuddin, S., and Moet, A. (1994). Reduction of residual stress in montmorillonite/epoxy compounds. Journal of Materials Science, 29(9), 2274-2280.

48. Lee, D. C., and Jang, L. W. (1996). Preparation and characterization of PMMA–clay hybrid composite by emulsion polymerization.
49. Okamoto, M., Morita, S., and Kotaka, T. (2001). Dispersed structure and ionic conductivity of smectic clay/polymer nanocomposites. Polymer, 42(6), 2685-2688.
50. Biasci, L., Aglietto, M., Ruggeri, G., and Ciardelli, F. (1994). Functionalization of montmorillonite by methyl methacrylate polymers containing side-chain ammonium cations. Polymer, 35(15), 3296-3304.
51. Akelah, A., El-Deen, N. S., Hiltner, A., Baer, E., and Moet, A. (1995). Organophilic rubber-montmorillonite nanocomposites. Materials Letters, 22(1-2), 97-102.
52. Paul, D. R., and Barlow, J. W. (1980). Polymer blends. Journal of Macromolecular Science—Reviews in Macromolecular Chemistry, 18(1), 109-168.
53. Xue, T. J., McKinney, M. A., and Wilkie, C. A. (1997). The thermal degradation of polyacrylonitrile. Polymer Degradation and Stability, 58(1-2), 193-202.
54. Ouyang, Q., Cheng, L., Wang, H., and Li, K. (2008). Mechanism and kinetics of the stabilization reactions of itaconic acid-modified polyacrylonitrile. Polymer Degradation and Stability, 93(8), 1415-1421.
55. Bahrami, S. H., Bajaj, P., and Sen, K. (2003). Effect of coagulation conditions on properties of poly (acrylonitrile–carboxylic acid) fibers. Journal of applied polymer science, 89(7), 1825-1837.
56. Bajaj, P., Sreekumar, T. V., and Sen, K. (2002). Structure development during dry–jet–wet spinning of acrylonitrile/vinyl acids and acrylonitrile/methyl acrylate copolymers. Journal of applied polymer science, 86(3), 773-787.

57. Liu, J. J., Ge, H., and Wang, C. G. (2006). Modification of polyacrylonitrile precursors for carbon fiber via copolymerization of acrylonitrile with ammonium itaconate. Journal of applied polymer science, 102(3), 2175-2179.

58. Devasia, R., Nair, C. R., Sadhana, R., Babu, N. S., and Ninan, K. N. (2006).

59. Ouyang, Q., Cheng, L., Wang, H., and Sun, Y. (2007). Study on thermal stabilization of poly (acrylonitrile-co-itaconic acid) by differential scanning calorimetry. ACTA CHIMICA SINICA-CHINESE EDITION-, 65(24), 2941.

60. Coleman, M. M., and Sivy, G. T. (1981). Fourier transform IR studies of the degradation of polyacrylonitrile copolymers I: introduction and comparative rates of the degradation of three copolymers below 200 C and under reduced pressure. Carbon, 19(2), 123-126.

61. Watt, W., and Johnson, W. (1975). Mechanism of oxidisation of polyacrylonitrile fibres. Nature, 257(5523), 210.

62. Fitzer, E., Frohs, W., and Heine, M. (1986). Optimization of stabilization and carbonization treatment of PAN fibres and structural characterization of the resulting carbon fibres. Carbon, 24(4), 387-395.

63. Fitzer, E., and Müller, D. J. (1975). The influence of oxygen on the chemical reactions during stabilization of pan as carbon fiber precursor. Carbon, 13(1), 63-69.

64. Tead, S. F., Kramer, E. J., Russell, T. P., and Volksen, W. (1990). Ion beam analysis of the imidization kinetics of polyamic ethyl ester. Polymer, 31(3), 520-523.

65. Koton, M. M., Kudriavtsev, V. V., and Svetlichny, V. M. (1984). Investigation of the reactivity of aromatic diamines and dianhydrides of tetracarboxylic acids in the synthesis of polyamic acids. In Polyimides (pp. 171-187). Springer, Boston, MA.

66. Bower, G. M., and Frost, L. W. (1963). Aromatic polyimides. Journal of Polymer Science Part A: General Papers, 1(10), 3135-3150.

67. Sroog, C. E., and Endrey, A. L. (1965). SV Abramo, CE Berr, WM Edward and KL Olivier, J. J. Polymer Sci., PartA, 3, p1378.

68. Chang, J., He, M., Niu, H., Sui, G., and Wu, D. (2016). Structures and properties of polyimide/polyacrylonitrile blend fibers during stabilization process. Polymer, 89, 102-111.

69. Rahaman, M. S. A., Ismail, A. F., and Mustafa, A. (2007). A review of heat treatment on polyacrylonitrile fiber. Polymer degradation and Stability, 92(8), 1421-1432.

70. Wangxi, Z., Jie, L., and Gang, W. (2003). Evolution of structure and properties of PAN precursors during their conversion to carbon fibers. Carbon, 41(14), 2805-2812.

71. Zhang, M., Zhao, X., Liu, W., He, M., Niu, H., and Wu, D. (2015). Effects of using polyacrylonitrile on the thermal, morphological and mechanical properties of polyimide/polyacrylonitrile blend fibers. Fibers and Polymers, 16(10), 2244-2250.

72. Damaceanu, M. D., Constantin, C. P., Bruma, M., and Belomoina, N. M. (2014). Highly fluorinated polyimide blends–Insights into physico-chemical characterization. *Polymer*, *55*(17), 4488-4497.

73. H.-L. Tyan, Y.-C. Liu, and K.-H. Wei, 1999.

74. Karamancheva, I., Stefov, V., Šoptrajanov, B., Danev, G., Spasova, E., and Assa, J. (1999). FTIR spectroscopy and FTIR microscopy of vacuum-evaporated polyimide thin films. *Vibrational spectroscopy*, *19*(2), 369-374.

75. Cetiner, S., Karakas, H., Ciobanu, R., Olariu, M., Kaya, N. U., Unsal, C., ... and Sarac, A. S. (2010). Polymerization of pyrrole derivatives on polyacrylonitrile matrix, FTIR–ATR

and dielectric spectroscopic characterization of composite thin films. *Synthetic Metals*, *160*(11-12), 1189-1196.

76. Farsani, R. E., Raissi, S., Shokuhfar, A., and Sedghi, A. (2009). FT-IR study of stabilized PAN fibers for fabrication of carbon fibers. *World Academy of Science, Engineering and Technology*, *50*, 430-433.
77. Ko, Tse-Hao, Hsing-Yie Ting, and Chung-Hua Lin. "Thermal stabilization of polyacrylonitrile fibers." Journal of applied polymer science 35.3 (1988): 631-640.
78. Zou, H., Wu, S., and Shen, J. (2008). Polymer/silica nanocomposites: preparation, characterization, properties, and applications. Chemical reviews, 108(9), 3893-3957.
79. Okafor, P. A., and Iroh, J. O. (2015).
80. Sanderson, Robert T. "Electronegativity and bond energy." Journal of the American Chemical Society 105.8 (1983): 2259-2261.
81. Pothan, L. A., George, C. N., John, M. J., and Thomas, S. (2010). Dynamic mechanical and dielectric behavior of banana-glass hybrid fiber reinforced polyester composites. *Journal of Reinforced Plastics and Composites*, *29*(8), 1131-1145.
82. Ramani, Ramasubbu, and Sarfaraz Alam. "Free volume and damping in a miscible high-performance polymer blend: Positron annihilation lifetime and dynamic mechanical thermal analysis studies." Journal of Applied Polymer Science 133.6 (2016).
83. Megusar, Janez. "Low temperature fast-neutron and gamma irradiation of Kapton® polyimide films." Journal of nuclear materials 245.2-3 (1997): 185-190.
84. Andrews, R. D., and R. M. Kimmel. "Solid state structure and glass transitions in polyacrylonitrile: The hetero-bonded solid state." Journal of Polymer Science Part B: Polymer Letters 3.3 (1965): 167-169.

85. Geethamma, V. G., Asaletha, R., Kalarikkal, N., and Thomas, S. (2014). Vibration and sound damping in polymers. *Resonance*, *19*(9), 821-833.

86. Ratna, D. "Handbook of Thermoset Resins; Smithers, Rapra." Technology: London, UK (2009).

87. Menrad, K. P. "Dynamic Mechanical Analysis: A Practical Introduction." (2008).

88. Nair, KC Manikandan, Sabu Thomas, and Gabriël Groeninckx. "Thermal and dynamic mechanical analysis of polystyrene composites reinforced with short sisal fibres." Composites Science and Technology 61.16 (2001): 2519-2529.

89. Goertzen, William K., and M. R. Kessler. Composites Part B: Engineering 38.1 (2007): 1-9.

90. Brostow, W., Chiu, R., Kalogeras, I. M., and Vassilikou-Dova, A. (2008). Prediction of glass transition temperatures: Binary blends and copolymers. *Materials Letters*, *62*(17-18), 3152-3155.

91. Koleske, J. V., and R. D. Lundberg. "Lactone polymers. I. Glass transition temperature of poly-ε-caprolactone by means on compatible polymer mixtures." Journal of Polymer Science Part A-2: Polymer Physics 7.5 (1969): 795-807.

92. Perera, MC Senake, U. S. Ishiaku, and ZA Mohd Ishak. "Characterisation of PVC/NBR and PVC/ENR50 binary blends and PVC/ENR50/NBR ternary blends by DMA and solid-state NMR." European Polymer Journal 37.1 (2001): 167-178.

93. Coats, A. W., and J. P. Redfern. "Thermogravimetric analysis. A review." Analyst 88.1053 (1963): 906-924.

94. Grassie, N., and R. McGuchan. "Pyrolysis of polyacrylonitrile and related polymers—I. Thermal analysis of polyacrylonitrile." European polymer journal 6.9 (1970): 1277-1291.

95. Xue, T. J., McKinney, M. A., and Wilkie, C. A. (1997). The thermal degradation of polyacrylonitrile. Polymer Degradation and Stability, 58(1-2), 193-202.

96. Agag, T., T. Koga, and T. Takeichi. "Studies on thermal and mechanical properties of polyimide–clay nanocomposites." Polymer 42.8 (2001): 3399-3408.

97. Chang, J., He, M., Niu, H., Sui, G., and Wu, D. (2016). Structures and properties of polyimide/polyacrylonitrile blend fibers during stabilization process. *Polymer*, *89*, 102-111.

98. Compendium, Modulated DSCTM. "Basic Theory and Experimental Considerations." TA Instruments Inc., New Castle, DE, USA, TA-210 (1996).

99. Chang, J., He, M., Niu, H., Sui, G., and Wu, D. (2016). Structures and properties of polyimide/polyacrylonitrile blend fibers during stabilization process. *Polymer*, *89*, 102-111.

100. Kurmvanshi, S. K., Gupta, A. K., Patel, P. R., Bajpai, R., and Keller, J. M. (2008). PAN based quasi carbon whiskers reinforced PI polyblends: Microhardness, mechanical, hydraulic, and morphological study. Polymer Engineering and Science, 48(3), 505-510.

101. Xiao, S., Wang, B., Zhao, C., Xu, L., and Chen, B. (2013). Influence of oxygen on the stabilization reaction of polyacrylonitrile fibers. Journal of Applied Polymer Science, 127(3), 2332-2338.